Predeployment Progress of the Canister Deposition Field Demonstration

Spent Fuel and Waste Disposition

Prepared for
US Department of Energy
Spent Fuel and Waste Science and Technology

D.G. Fascitelli and S.G. Durbin
Sandia National Laboratories, Albuquerque, NM

May 26, 2023
Milestone No. M2SF-23SN010208034
SAND2023-04194 R

Sandia National Laboratories
U.S. DEPARTMENT OF ENERGY NNSA

Sandia National Laboratories is a multimission laboratory managed and operated by National Technology & Engineering Solutions of Sandia, LLC, a wholly owned subsidiary of Honeywell International Inc., for the U.S. Department of Energy's National Nuclear Security Administration under contract DE-NA0003525.

DISCLAIMER

This information was prepared as an account of work sponsored by an agency of the United States Government. Neither the United States Government nor any agency thereof, nor any of their employees, nor any of their contractors, subcontractors, or their employees, make any warranty, expressed or implied, or assumes any legal liability or responsibility for the accuracy, completeness, or usefulness, of any information, apparatus, product, or process disclosed, or represents that its use would not infringe privately owned rights. References herein to any specific commercial product, process, or service by trade name, trademark, manufacturer, or otherwise, does not necessarily constitute or imply its endorsement, recommendation, or favoring by the United States Government, any agency thereof, or any of their contractors or subcontractors. The views and opinions of authors expressed herein do not necessarily state or reflect those of the United States Government, any agency thereof, or any of their contractors.

Prepared by
Sandia National Laboratories
Albuquerque, New Mexico 87185 and Livermore, California 94550

Sandia National Laboratories is a multi-mission laboratory managed and operated by National Technology & Engineering Solutions of Sandia, LLC, a wholly owned subsidiary of Honeywell International, Inc., for the U.S. Department of Energy's National Nuclear Security Administration under contract DE-NA0003525.

ABSTRACT

This report updates the high-level test plan for evaluating surface deposition on three commercial 32PTH2 spent nuclear fuel (SNF) canisters inside NUTECH Horizontal Modular Storage (NUHOMS) Advanced Horizontal Storage Modules (AHSMs) from Orano (formerly Transnuclear Inc.) and provides a summary of the surface sampling activities that have been conducted to date. The details contained in this report represent the best designs and approaches explored for testing as of this publication. Given the rapidly developing nature of this test program, some of these plans may change to accommodate new objectives or requirements.

One goal of this testing is to collect defensible and detailed dust deposition measurements from the surface of dry storage canisters in a marine coastal environment to guide chloride-induced stress corrosion cracking (CISCC) research. Another goal is to provide data for the validation of computational fluid dynamics (CFD) based deposition modeling. To facilitate surface sampling, the otherwise highly prototypic dry storage systems will not contain SNF but rather will be electrically heated to mimic the decay heat and thermal-hydraulic environment. Test and heater design is supported by detailed CFD modeling. Instrumentation throughout the canister, storage module, and environment will provide extensive information about the thermal-hydraulic behavior of horizontal dry cask storage systems. Manual sampling over a comprehensive portion of the canister surface at regular time intervals will offer detailed quantification and composition of the deposited particulates from a realistic storage environment.

Discussions of a potential host site for the Canister Deposition Field Demonstration (CDFD) are ongoing. Until a host site is chosen, testing of key CDFD hardware components including the heater assemblies, power skid, and remote data acquisition system will continue. Functional testing of the finalized heater assemblies and test apparatus started this fiscal year. These initial heater tests have shown the assemblies are performing within design specifications. Staged surface sampling of a mockup of a canister outside the AHSM on a transfer skid was also performed. Refinements to the sampling procedures and techniques were captured from observation of these activities and lessons-learned debriefs. These updated sampling procedures and techniques are planned to be tested again in the field using the mockup in order to assure personnel are using the most accurate and repeatable methods possible prior to deployment for actual CDFD testing.

This page is intentionally left blank.

ACKNOWLEDGEMENTS

This work was funded by the U.S. Department of Energy, Office of Nuclear Energy Spent Fuel and Waste Disposition Research and Development Program.

The authors would like to express their appreciation to Ned Larson of the Department of Energy for his programmatic leadership and vision. The authors would also like to recognize the internal support and leadership from Sylvia Saltzstein, Geoff Freeze, Stephanie Booth, and Scott Sanborn of Sandia National Laboratories. Progress on this project would not be possible without the hard work of the Nuclear Energy Work Complex technologist team. The authors would also like to recognize Sarah Suffield and Ben Jensen of Pacific Northwest National Laboratories (PNNL) for their efforts with the thermal and deposition modeling. Finally, the authors would like to acknowledge the valued collaboration from Steve Ross and Brady Hanson of PNNL.

This page is intentionally left blank.

CONTENTS

LIST OF FIGURES

This page is intentionally left blank.

LIST OF TABLES

This page is intentionally left blank.

EXECUTIVE SUMMARY

As spent nuclear fuel (SNF) pools continue to operate at or near capacity, dry cask storage systems provide the solution for additional storage of spent fuel. Without a permanent means of disposal for SNF in the United States, the nation's stockpile of spent fuel in interim storage continues to grow. Systems that were originally licensed by the United States Nuclear Regulatory Commission for up to 40 years have remained in service longer than expected, which has raised unanticipated concerns. Stress corrosion cracking is a known concern for these systems that requires the action of three interdependent variables—a tensile stress, a susceptible material, and the presence of a corrosive species. The residual stresses introduced by welding during fabrication of the canisters creates local stresses that are capable of causing stress corrosion cracking, and the stainless steels common to spent fuel canister shells are known to be susceptible. Over time, dust particulates from the ambient containing corrosive salts deposit on the canister surface. As the spent fuel canister cools, these salts may form concentrated brines with moisture absorbed from the ambient air and complete the required conditions for stress corrosion cracking to be possible.

The objective of this study is to reliably measure and quantify the deposition of corrosive species (chloride salts) from marine coastal ambient air onto prototypic SNF canisters. To facilitate surface sampling, the otherwise highly prototypic dry cask storage systems will not contain SNF but rather will be electrically heated to mimic the decay heat and thermal environment. The study will include three identically instrumented dry cask storage systems, powered at three distinct heat loads. One system will represent a canister loaded with roughly the maximum allowed heat load (40 kW), another loaded with one quarter of the maximum heat load (10 kW), and the third with no heat applied as a control (0 kW).

Preliminary heater tests have been conducted at heat loads ranging from 4.8 to 35.0 kW. Figure E.1 presents thermal images taken during a test at a total applied heat load of 20.0 kW. Preliminary heater tests indicated that the electric heaters are appropriate surrogates for spent nuclear fuel and can adequately heat the canister shell to match the temperatures expected for SNF-loaded canisters. Initial testing has also informed thermal modeling parameters and facilitated the development of a more accurate thermal model of the system.

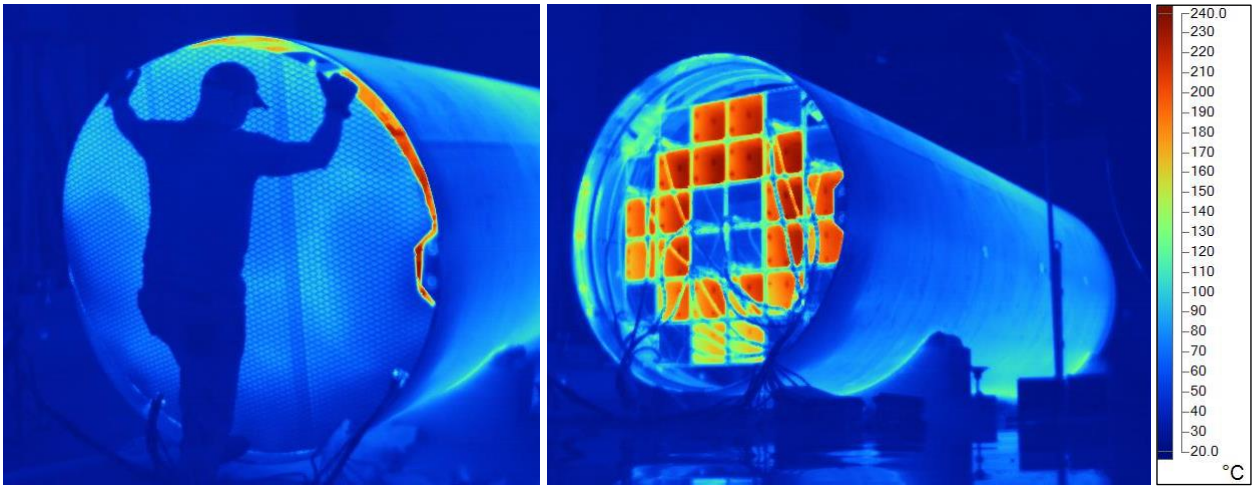

Figure E.1 Thermal images of the removal of the thermal radiation shield (left) and electrically heated canister (right) during a preliminary heater test performed at 20.0 kW total heat load.

Heater assemblies have been redesigned and will fully populate all thirty-two basket cells of each canister. Heater assemblies are currently being instrumented with thermocouples at various locations of interest to develop a thermal profile of the canister interior. Testing of these assemblies will begin later this fiscal year. Additional testing will continue to support thermal modelling efforts.

Mockup structures of the canister transfer skid and Advanced Horizontal Storage Module (AHSM) rear wall were designed and built at the Nuclear Energy Work Complex in Sandia National Laboratories. These mockups provide a realistic setting for the surface sampling and testing teams to establish proper operational procedures and identify any limitations or obstacles of the testing setup and equipment. Figure E.2 shows images taken during a practice surface sampling activity. In the images, staff collect deposits with a plastic template and wetted sponges from a lab-prepared plate fixed to the canister. The purpose of this activity was to establish a proper sampling procedure, familiarize the sampling team with the equipment that will be used in the field, assess the accessibility of the canister surface while on the transfer skid, and evaluate the efficiency of the sampling method.

Figure E.2 Lab-prepared sheet metal plates coated with known quantities of salt were mounted on a spent fuel canister and sampled by hand from an articulated boom lift. The canister was positioned on top of the transfer skid mockup at prototypic height for this testing.

The Canister Deposition Field Demonstration project is a large-scale test with highly prototypic dry cask storage system components. The project is slated to last several years to collect highly defensible and detailed dust deposition measurements from the surface of dry storage canisters in a marine coastal environment to guide chloride-induced stress corrosion crack research. The proposed testing layout of the three storage modules and a canister extracted for sampling activities is shown in Figure E.3.

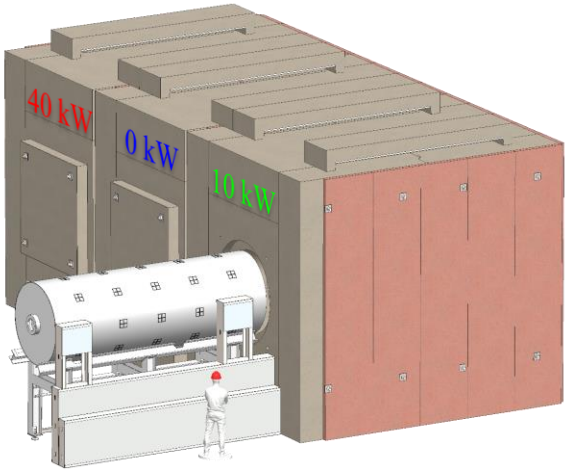

Figure E.3 Testing layout of the AHSMs and canister during sampling procedures.

ACRONYMS

AHSM	Advanced Horizontal Storage Module
AMPs	aging management programs
C-DAQ	CompactDAQ
CDFD	Canister Deposition Field Demonstration
DAQ	data acquisition
DCSS	dry cask storage system
DOE	U.S. Department of Energy
DSC	dry shielded canister
FY	fiscal year
FSAR	Final Safety Analysis Report
HLZ	heat load zone
HVAC	heating, ventilation, and air conditioning
ISFSI	independent spent fuel storage installation
NE	Office of Nuclear Energy
NI	National Instruments
NEWC	Nuclear Energy Work Complex
NRC	United States Nuclear Regulatory Commission
NUHOMS	NUTECH Horizontal Modular Storage
OTC	outer top cover
PHT	peak heater temperature
PNNL	Pacific Northwest National Laboratory
PWR	pressurized water reactor
PXI-e	peripheral component interconnect extensions for instrumentation - express
RDP	remote desktop protocol
SCC	stress corrosion crack
SCR	silicon-controlled rectifier
SFWD	Spent Fuel and Waste Disposition
SNF	spent nuclear fuel
SS	stainless steel
TC	thermocouple
VPN	virtual private network

This page is intentionally left blank.

PREDEPLOYMENT PROGRESS OF THE CANISTER DEPOSITION FIELD DEMONSTRATION

This report fulfills milestone M2SF-23SN010208034 in the Canister Deposition Field Demonstration (CDFD) work package (SF-23SN01020803). This work is sponsored under the Department of Energy's (DOE) Office of Nuclear Energy (NE) Spent Fuel and Waste Disposition (SFWD) campaign.

1 INTRODUCTION

Dry cask storage systems (DCSSs) for spent nuclear fuel (SNF) are designed to provide a confinement barrier that prevents the release of radioactive material to its surroundings, maintain SNF in an inert environment, provide radiation shielding, and maintain subcriticality conditions. After fuel has been used in a commercial nuclear reactor and is no longer economically viable for power generation, the fuel is considered "spent" and relocated from the reactor to a SNF pool. Despite the fission reaction being stopped, the SNF is radioactive and continues to release heat as the fission products decay. Spent fuel pools provide radiation shielding and cool the spent fuel assemblies, which continue to generate heat for years after removal from the reactor. After sufficient cooling in the pools, the SNF is loaded into a dry shielded canister (DSC) and placed inside of a transfer cask. The DSC is welded shut and undergoes a vacuum drying procedure to evacuate nearly all the water from the system. The DSC is pressurized, or backfilled, with an inert gas, typically helium, and then moved to an on-site dry storage location for interim storage. An independent spent fuel storage installation (ISFSI) is designed for interim storage of SNF, reactor-related greater than Class C waste, and other associated radioactive materials. Figure 1.1 presents a representation of an ISFSI pad containing horizontal dry cask storage systems. Figure 1.2 shows the major components of both horizontal and vertical dry cask storage systems for SNF.

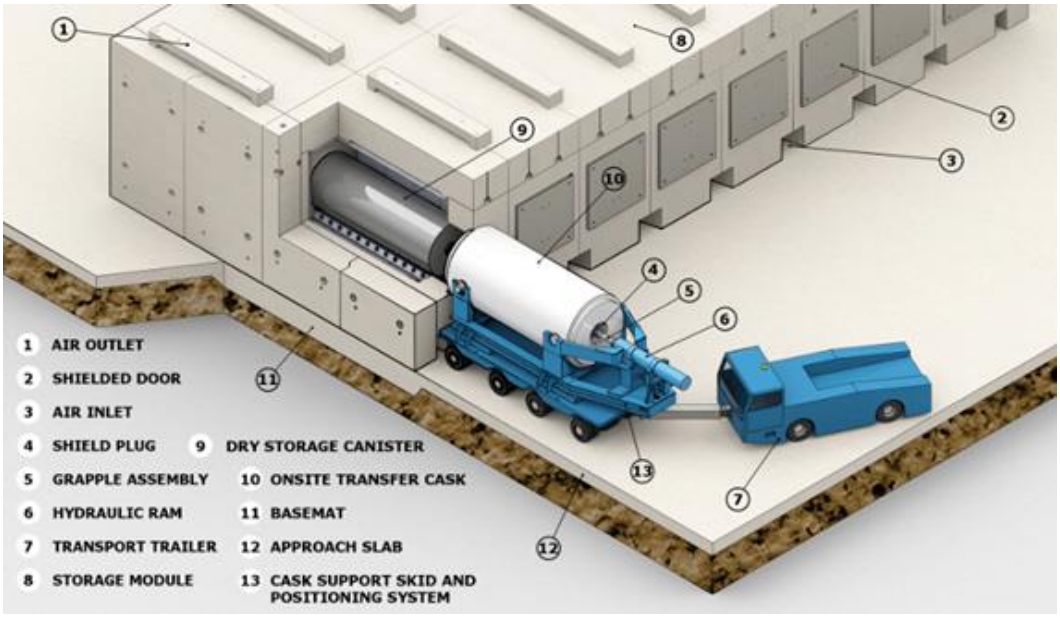

Source: https://www.orano.group/usa/en/our-portfolio-expertise/used-fuel-management/used-

Figure 1.1 Representation of a typical horizontal dry cask system located on an ISFSI pad.

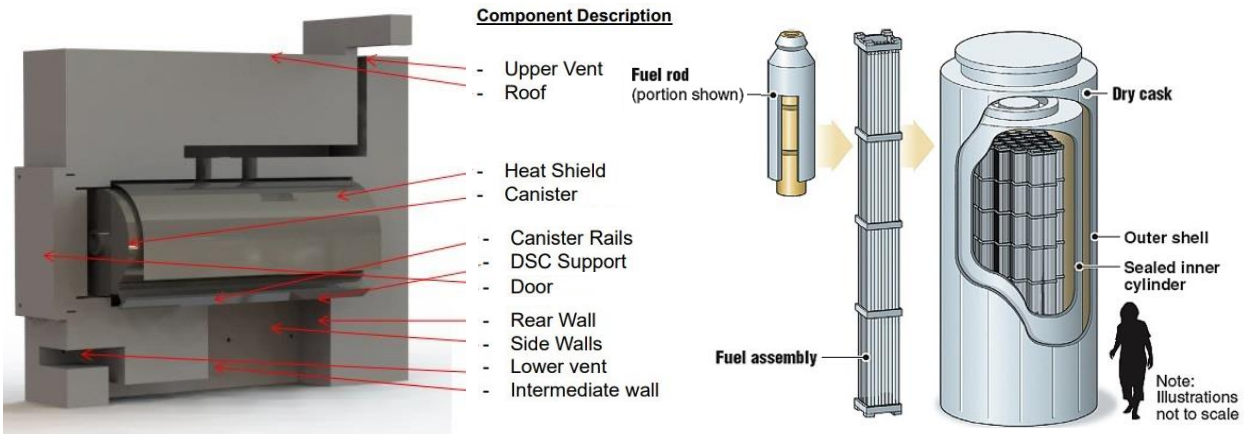

Source: https://twitter.com/Orano_usa/status/1174384799181692930/photo/1

Source: Exelon Corp., Westinghouse Electric Co., U.S. Nuclear Regulatory Commission

Figure 1.2 Major components of typical horizontal—left and vertical—right dry cask storage systems.

With SNF pools operating at or near capacity, DCSSs provide a solution for extended storage. Without a permanent means of disposal for SNF in the United States, the nation's stockpile of SNF in interim dry cask storage continues to grow. Systems that were designed for short term storage, and originally licensed by the United States Nuclear Regulatory Commission (NRC) for up to 40 years, have remained in service for times longer than expected, which could present a problem.

Typically, DSCs are made of stainless steel (SS). Dry cask storage systems are designed with an open volume between the DSC and storage module or cask. These systems are passively cooled by natural convection, drawing in ambient air from inlets at the bottom to outlets at the top. This reliance on the natural convection of ambient air to cool the system allows dust and other particulates from the environment into the DCSS. These particulates may then settle and collect on the surfaces of the canister. As the SNF cools over time, salts contained in the dust may deliquesce in the presence of moisture from the ambient relative humidity to form concentrated brines, which may contain corrosive species such as chlorides. These species can cause localized corrosion, called pitting. With sufficient tensile stresses, these pits can evolve into stress corrosion cracks (SCCs), which could penetrate through the canister wall and allow communication from the interior of the canister to the external environment [Schindelholz, 2017].

The NRC has implemented aging management programs (AMPs) aimed to prevent and mitigate aging effects, such as the development of SCCs, and establish a monitoring program to inspect DSCs for indications of aging. Efforts to assess and address materials aging issues for extended storage of SNF are ongoing. Stress corrosion cracking requires the action of three interdependent variables—a tensile stress, a susceptible material, and the presence of a corrosive species [U.S.NRC, 2011]. The residual stresses caused from welding during fabrication of the DSCs may provide local stresses that are conducive to stress corrosion cracking, and stainless steel is known to be a susceptible material. The quantity and chemistry of corrosive species on the canister surface in a realistic environment is currently the variable with the most uncertainty.

Current surface sampling techniques for DSCs loaded with SNF are unvalidated. A common technique for inspection and deposition sampling employs robotic devices to collect samples from the canister surface. The use of robotic sampling allows the sampling team to sample remotely and ensure minimal exposure to radiation from the SNF-loaded DSCs. Such methods provide qualitative measurements of the salt and dust composition on the canister surface. However, the quantitative accuracy of these techniques has not been validated and therefore the efficiency of robotic sampling is unknown. Typical robotic sampling methods

utilize vacuum suction approaches to traverse the canister surface, which will not be feasible with very high dust deposition loads. These robotic devices will also disturb the surface dusts not intended to be collected and interfere with future surface sampling plans. Figure 1.3 shows an example of a robotic sampling device from Robotic Technologies of Tennessee that was used to inspect and collect dust deposition from a DCSS canister.

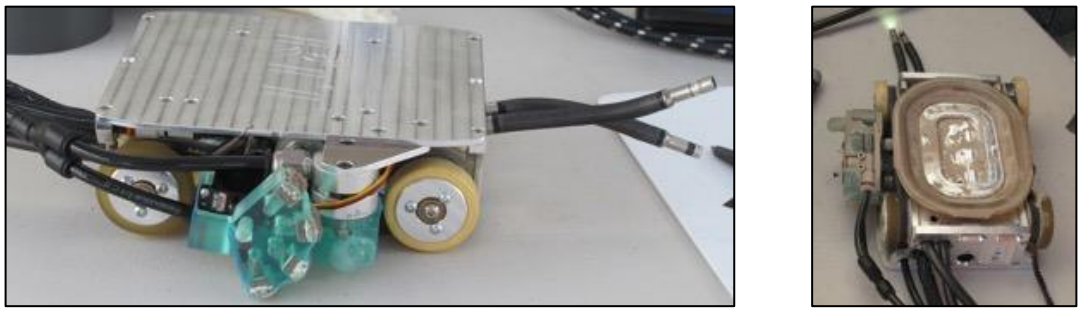

Figure 1.3 Example of a remote-operated robotic canister surface sampling device before (left) and after (right) canister surface sampling from Robotic Technologies of Tennessee.

1.1 Objective

This report provides updates on the high-level test plan [Lindgren *et al*., 2020] and previous status update [Fascitelli *et al*., 2022] for the CDFD project, specifically for evaluating surface deposition on DSCs and the continued work in preparation for canister deployment to a remote host site. The objective of this study is to reliably measure and quantify the deposition of corrosive species (chloride salts) from marine coastal ambient air onto prototypic SNF canisters. To facilitate surface sampling, the otherwise highly prototypic DCSSs will not contain SNF but rather will be electrically heated to mimic the decay heat and thermal environment.

The study will include three identical DCSSs. One system will represent a canister loaded with roughly the maximum allowed heat load (40 kW), another will represent a canister loaded with one quarter of the maximum heat load (10 kW), and the third canister will be used as an unheated control (0 kW).

The DOE-NE SFWD campaign has provided three Orano (formerly Transnuclear Inc.) NUTECH Horizontal Modular Storage (NUHOMS) 32PTH2 dry shielded canisters and Advanced Horizontal Storage Modules (AHSMs) for use in the study, illustrated in Figure 1.4. The 32PTH2 canister can hold thirty-two pressurized water reactor (PWR) fuel assemblies. The three canisters were delivered to Sandia National Laboratories (SNL) on November 13, 2020. Figure 1.5 shows a photograph of the three canisters staged in the high bay of Sandia's Building 6630 where they have been fitted with electrical heaters and instrumented with thermocouples for the preliminary heater testing outlined in Section 3.2. Discussions are ongoing to locate a suitable facility to host this long-term deposition study. An ISFSI near a marine coastal environment would be ideal to provide harsh yet realistic conditions.

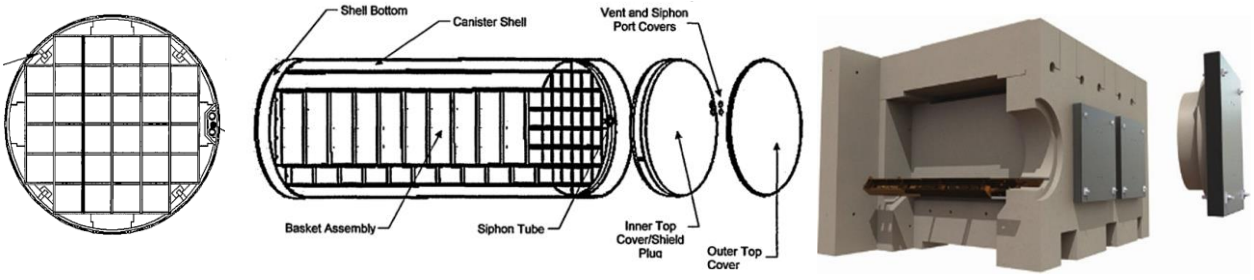

Figure 1.4 32PTH2 dry shielded canister (end view—left, side view—center) and Advanced Horizontal Storage Modules (sectioned side view—right).

Figure 1.5 Three 32PTH2 spent fuel canisters located inside of SNL's Building 6630 south high bay for preliminary heater testing.

The three canisters will be designed to simulate three decay heats. Figure 1.6 shows the proposed test setup with three electrically powered canisters and storage modules.

1. 0 kW decay heat for control. Canister will be loaded with heater assemblies and insulation to perform as a backup if other systems fail. The control canister should be most susceptible to deliquescence due to having the coolest surface temperatures.
2. 10 kW decay heat to represent canisters that have been stored for a while and more susceptible to deliquescence than the higher-powered canister because of cooler surface temperatures.
3. 40 kW decay heat to represent a freshly loaded system with short-cooled fuel. The decay heat will be decreased at various intervals to determine how concentration, composition, and location of deposits vary with decay heat and associated air flow velocities and patterns.

After some period of time to be determined based on a combination of modeling and ambient aerosol host site characterization, the canisters will be inspected for salt composition and concentration at various locations on the canister surface as described in Section 2.4.1.

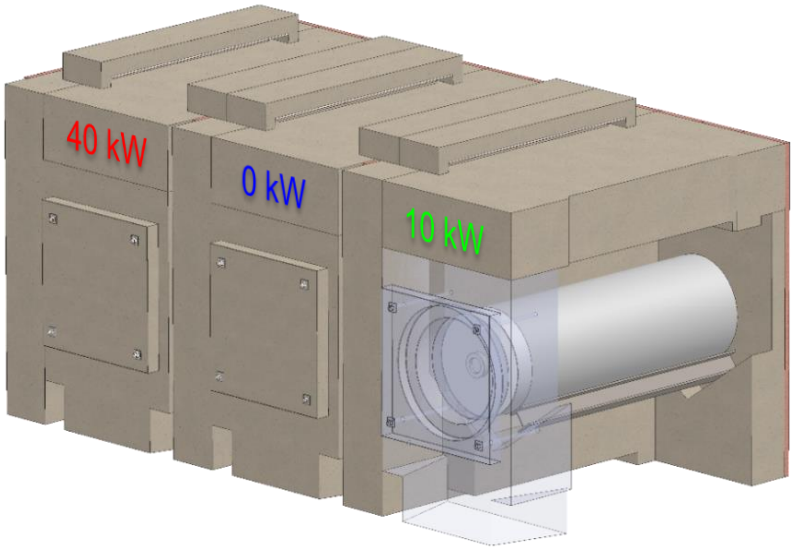

*AHSM end wall hidden to reveal dry storage canister inside.

Figure 1.6 Experimental test setup with three AHSMs with their respective dry shielded canisters electrically powered to 0, 10, and 40 kW.

2 APPARATUS AND PROCEDURES

The 32PTH2 canisters were selected for testing based on availability and suitability. Five of these canisters were made available to Sandia National Laboratories by the DOE-NE SFWD campaign for research purposes, with three designated for the CDFD project. While the 32PTH2 is not the latest generation of canister designs, the technology contained in this system is representative of the domestic fleet of DSCs, especially for horizontal dry cask storage systems.

2.1 32PTH2 Dry Shielded Canister

The prototypic DSC top shield plug assembly consists of the shield plug, inner top cover, and outer top cover (OTC). The shield plug provides radiation shielding from SNF and will not be required because the heat source is not radioactive. The shield plug is nominally 14 cm (5.5 in.) thick ASTM A36 carbon steel, weighs about 2,900 kg (6,380 lbs.) and typically rests on a support ring welded to the inside circumference of the canister. In prototypic commercial application, both the inner and outer top covers are welded in place to produce redundant hermetic seals, which are also not needed for the proposed testing. Both the inner and outer top covers are nominally 5 cm (2 in.) thick and weigh about 1,000 kg (2,200 lbs.). The outer diameter of the OTC is roughly 4.5 mm (0.18 in.) smaller than that of the shield plug and inner top cover. The inner top cover is made of SS304 and the outer top cover is made of SS316, the same material as the canister shell. For CDFD testing, the outer top cover will serve as the only top closure component installed. The increased resistance to chloride attack in marine environments of SS316 compared to SS304 is the main justification for choosing the OTC for our design. Figure 2.1 illustrates some details of the prototypic and test DSC top closure assemblies. When installed, the OTC will rest on the shield plug support ring.

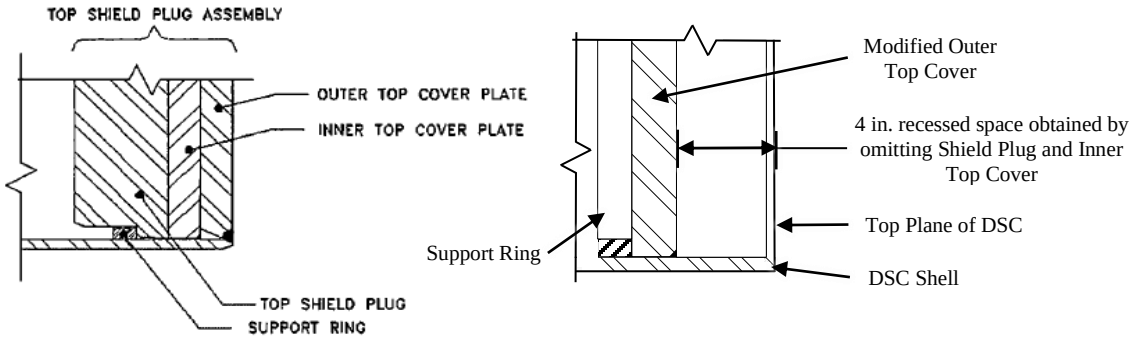

Figure 2.1 Detail of the prototypic top closure assembly (left) and CDFD top closure assembly (right) for a 32PTH2 canister. Left adapted from Figure B.3.1-1 [Transnuclear, 2016].

The recessed space obtained by locating the OTC on the shield plug support ring will allow approximately 10 cm (4 in.) of space below the top plane of the canister shell for the power junction box to be mounted. This design feature ensures the power junction box will not interfere with the canister insertion into the AHSM. The installation of a thin insulation layer on the OTC is being considered to provide additional protection to the components within the junction boxes and to simulate the conductive losses of the shield plug and inner cover plate. Further modeling is needed to determine if additional insulation on the OTC will improve comparisons with prototypic canister temperatures.

The component weights for a prototypic 32PTH2 spent fuel canister are provided in Table 2.1. With the elimination of the shield plug and inner top cover, and substitution of electric heater assemblies for spent nuclear fuel, the loaded CDFD test canisters will be about half as heavy as a prototypic SNF-loaded canister. The component weights of the CDFD test canisters are provided in Table 2.2.

Table 2.1 The components and respective weights of a prototypic 32PTH2 dry shielded canister and spent nuclear fuel assemblies are presented below [Transnuclear, 2017].

Component	Nominal Weight	
	Pounds	Kilograms
Canister shell and bottom end assembly	13,335	6,048
Outer top cover plate	2,140	971
Inner top cover plate	2,150	975
Top shield plug and support ring	6,430	2,916
Total canister assembly	**24,055**	**10,909**
Fuel compartments (32)	11,090	5,030
Aluminum/poison plates	4,920	2,231
Stainless steel plates	2,360	1,070
Small support rails	3,260	1,479
Large support rails	9,370	4,250
Basket fuel spacer assembly	1,460	662
Total fuel basket assembly	**32,460**	**14,721**
Total empty DSC (basket and canister)	56,515	25,630
SNF assembly (×32) at 1610 lbs./assembly	51,520	23,365
Total SNF-loaded DSC weight	**108,035**	**48,995**

Table 2.2 The components and respective weights for the CDFD 32PTH2 dry shielded canister system and heater assemblies are presented below.

Component	Nominal Weight	
	Pounds	Kilograms
Canister shell and bottom end assembly	13,335	6,048
Outer top cover plate	2,140	971
Cross brace	220	100
Total canister assembly	**15,695**	**7,118**
Fuel compartments (32)	11,090	5,030
Aluminum/poison plates	4,920	2,231
Stainless steel plates	2,360	1,070
Small support rails	3,260	1,479
Large support rails	9,370	4,250
Basket fuel spacer assembly	1,460	662
Total fuel basket assembly	**32,460**	**14,721**
Total empty DSC (basket and canister)	48,155	21,839
Heater assembly (×32) at 80 lbs./assembly	2,560	1,161
CDFD total loaded DSC weight	**50,715**	**23,000**

2.1.1 Cross Brace Installation

The basket assembly within a DSC segregates the loaded SNF assemblies but is not mechanically captured within the DSC. A cross brace is installed in an empty DSC to prevent any potentially damaging shifting or sliding of the basket assembly during transportation. The cross brace, shown in Figure 2.2, attaches to the DSC via the lifting lugs near the top support ring and sits flush against the basket assembly. The cross brace will serve its traditional purpose of securing the basket assembly, as well as protecting the electrical heaters from damage during transportation of the DSCs to the host site.

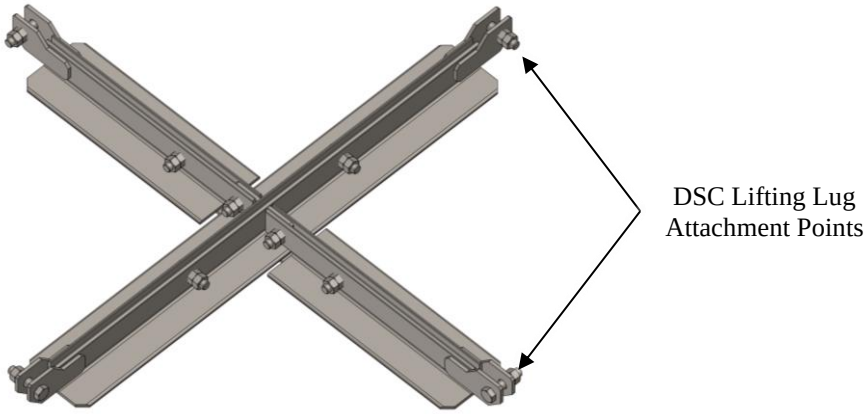

Figure 2.2 Computer model of DSC cross brace.

Laser line surface scanning was performed to characterize the shape of the canisters. This process is a non-contact method of measuring the shape of a 3-dimensional object. The results of the laser line surface scanning on the 32PTH2 canisters were presented in the previous status update for the canister deposition field demonstration [Lindgren *et al*., 2021]. The data was referenced to a primitive cylinder to produce the displacement differences (*i.e.*, deviations from a perfect cylinder) shown in Figure 2.3 with a range of ± 3.2 mm (± 0.125 in.) on the color scale. This displacement occurs from deformation of the shell due to the weight of the DSC and a lack of support, due to the absence of the top closure assembly, at the open end. Typically, DSCs are loaded with spent fuel and the covers are installed when the canister is in a vertical orientation and this deformation is avoided. The CDFD canisters will be loaded with electric heaters and the OTC will be installed when the canister is horizontal. Before final installation of the OTC, the cross brace will be installed to help maintain a circular cross section at the opening where deformation is greatest.

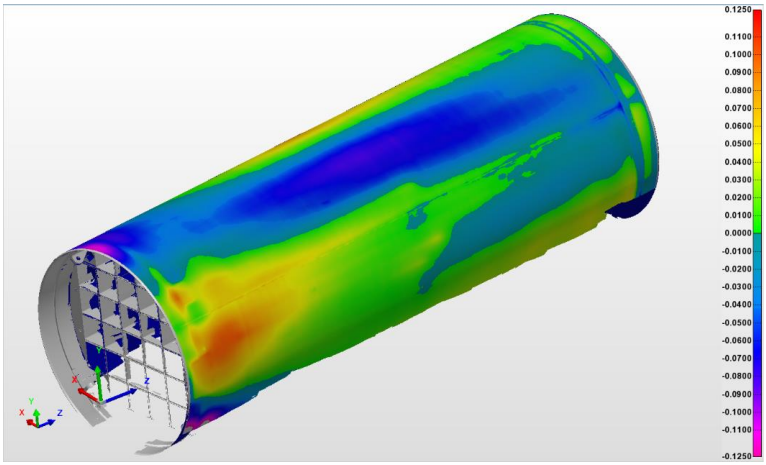

Figure 2.3 Displacement differences from primitive cylinder in inches [Lindgren *et al*., 2021].

The deformation of the DSC from its own weight is purely elastic. When lifted from the support cradle, the shell returns to a circular cross-section. A dry fit of the cross brace was executed to evaluate its ability to maintain a circular cross-section at the canister opening when the canister is rested horizontally. Horizontal and vertical inner diameter measurements of the rested canister were taken with a laser range finder before and after the cross brace was installed. To install the cross brace, the open end of the canister was first lifted slightly with an overhead crane to ensure the canister was in round. The cross brace was then fastened to each of the four DSC lifting lugs and the additional bracing bolts were tightened. The canister was then placed back onto the cradle. Figure 2.4 shows the canister immediately after installation of the cross brace. The inner diameter measurements of the rested canister before, during, and after installation are presented in Table 2.3. Although the horizontal diameter of the shell was unaffected by the addition of the cross brace, the canister shell relaxed to have a vertical diameter about 1/32 in. larger after installation, which could benefit the installation of the OTC.

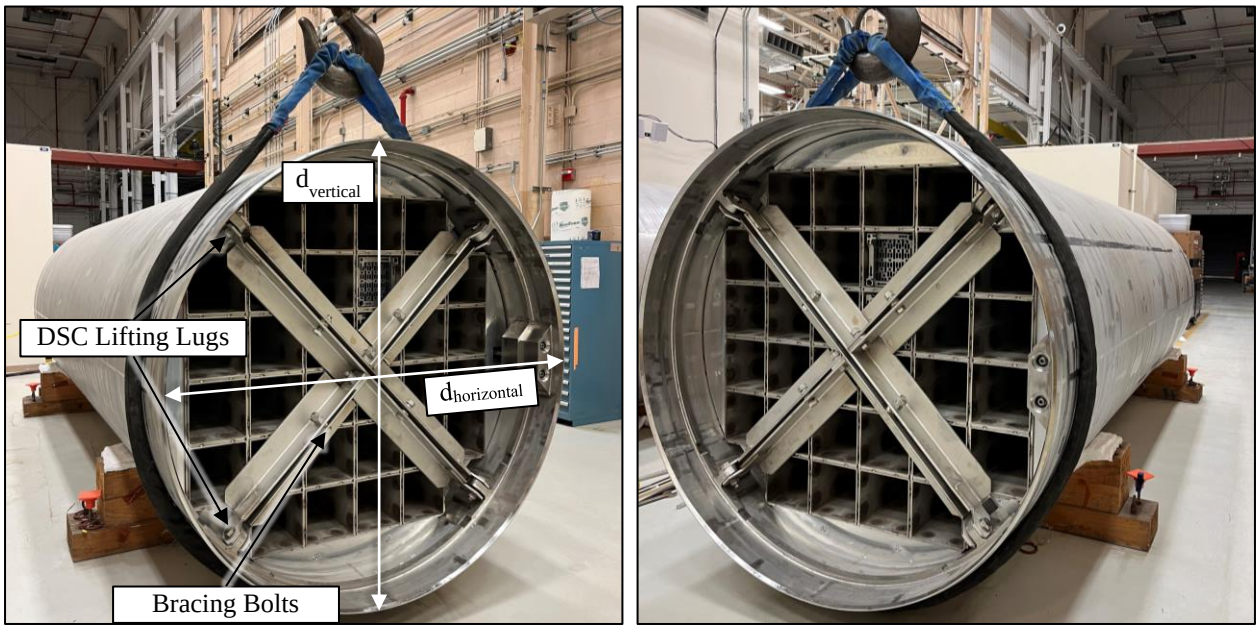

Figure 2.4 Cross brace dry fit to assess its ability to maintain a circular opening and ensure horizontal installation is feasible.

Table 2.3 Vertical and horizontal inner diameter measurements before, during, and after cross

DSC Orientation	$d_{vertical}$ (in.)	$d_{horizontal}$ (in.)
Rested DSC (no cross brace)	68.06	68.38
Choked DSC	68.25	68.25
Rested DSC (cross brace installed)	68.09	68.38

2.1.2 Modifications to DSC Outer Top Cover

The DSC outer top cover will serve as the only top closure component and is intended to be installed and left in place through the duration of testing. All modifications to the outer top cover are illustrated in Figure 2.5. The outer diameter of the OTC is 1,732 mm (68.20 in.). About 2.7 mm (0.11 in.) of interference from the OTC and canister shell will result from the deformation of the canister opening discussed previously. To ensure proper fit, material will be removed from the top and bottom of the cover, to a vertical diameter of 1,727 mm (68.0 in.).

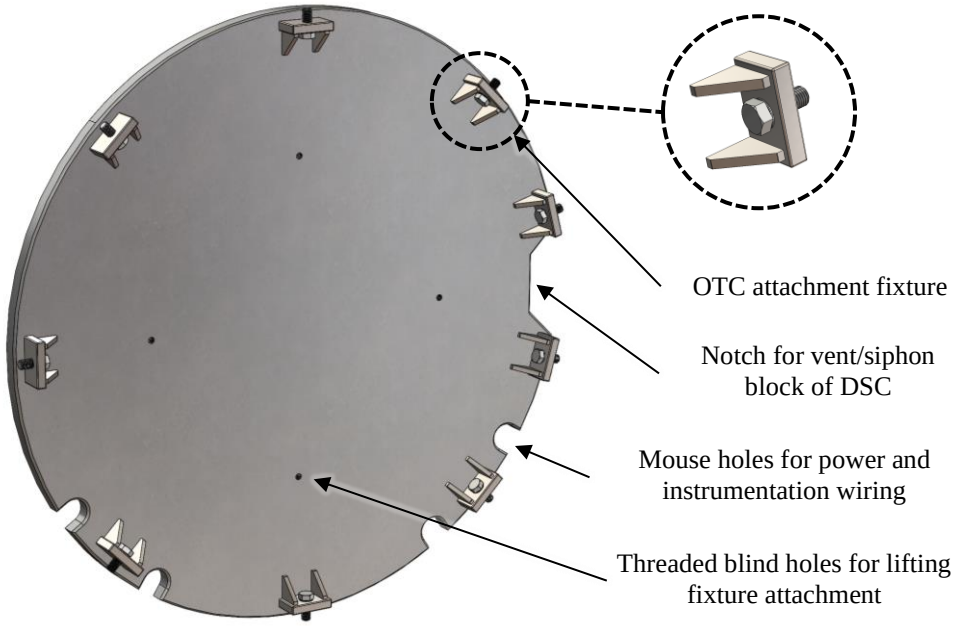

Figure 2.5 Modifications to the outer top cover to accommodate CDFD testing.

The electric heaters that simulate the decay heat of spent fuel and the internal thermocouples that monitor the thermal response require penetrations in the canister's outer top cover for signal and power wiring. Should maintenance or repair be required, the OTC will be removeable with the canister in its horizontal orientation. The initially proposed OTC attachment method involves mounting fixtures, installed circumferentially, to hold it in place during normal operations. The fixtures will function as set screws for the cover, applying a compressive force into the DSC shell to secure it. A more robust attachment method not reliant solely upon friction is being explored to ensure safe transport of the OTC, DSC, and the heater assemblies inside. To facilitate installation or removal, an OTC lifting fixture was designed and constructed [Lindgren *et al*., 2021]. Figure 2.6 shows the lifting fixture attached via bolts threaded into blind holes on the cover. The inner top cover is pictured in the photograph. The notch on the right side of the inner lid (as pictured) is to accommodate the vent/siphon block. The same dimension notch will be cut into the OTC.

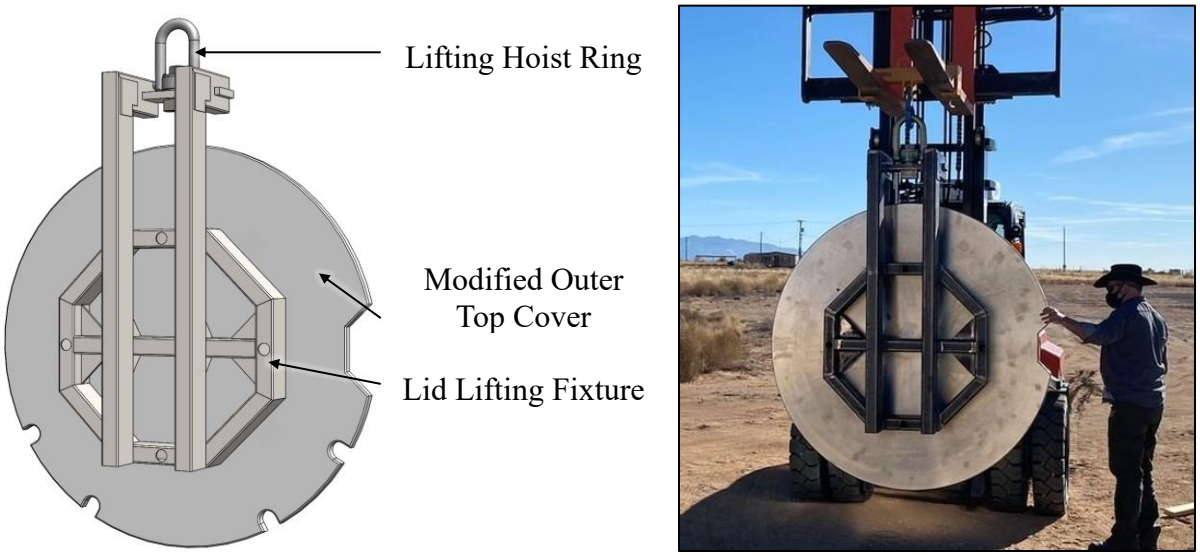

Figure 2.6 Lifting fixture allows OTC to be installed into canister horizontally.

An exploded view of a dry shielded canister in its horizontal orientation is shown in Figure 2.7. The cross brace will be installed to facilitate the security of the basket and heater assemblies during transportation and support the canister opening during installation of the OTC. The canister will be populated with 32 electric heater assemblies, as shown in Figure 2.7.

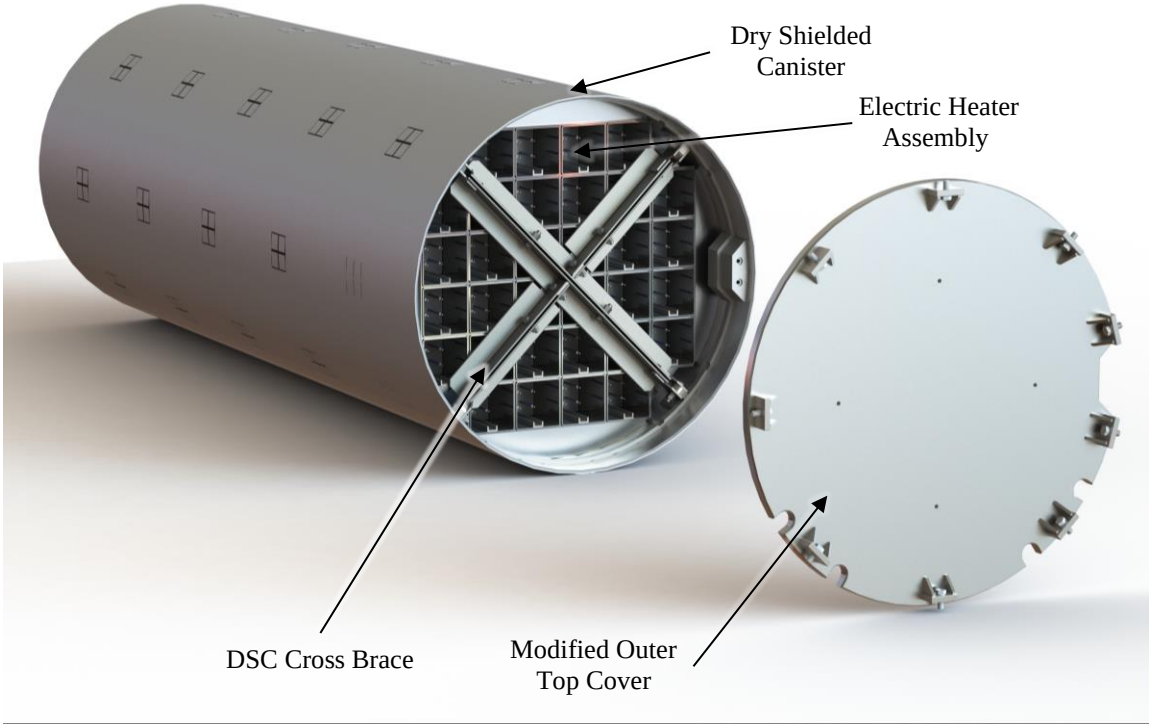

Figure 2.7 Exploded view of 32PTH2 canister with cross brace installed (left) and modified outer top cover (right). Canister loaded with electrical heater assemblies.

2.2 Advanced Horizontal Storage Module

After sufficient time to cool in the fuel pool, SNF assemblies are loaded into the DSC. The canister then undergoes a vacuum drying procedure to evacuate nearly all water from the system. Only when dryness criteria have been met is the DSC ready for dry storage. The DSC and its transfer cask are typically placed on a transfer skid (discussed in the subsection below) and the canister is loaded into the AHSM. The DSC will remain in the AHSM for a significant amount of time until a solution for the permanent disposal of SNF is realized.

2.2.1 Canister-AHSM Insertion and Extraction

Depending on the available facilities at the host site, a means for inserting and extracting the canister will need to be devised for the CDFD test. Figure 2.8 shows a typical transfer skid that is used for inserting and extracting spent fuel canisters into and out of the AHSM. A modified transfer skid is being explored in further detail and is the preferred choice. A mechanical drawing of the modified transfer skid is shown in Figure 2.9. The DSC will not need the shielding transfer cask, allowing access to most of the canister surface for sampling. The transfer skid will incorporate custom support rollers to facilitate canister movement and preservation of the surface deposition profile through reducing the vibration during extraction of the canister. These specialized support rollers should prevent marring of the bottom canister surface, potentially severely damaging the canister. The rollers will need to be notched out to accommodate lifting straps used in the placement of the canister onto the transfer skid prior to initial insertion into the AHSM vault. The support rails inside of the AHSM will be substituted with rollers as well to facilitate

canister insertion and extraction. Figure 2.10 shows a mechanical drawing of the roller rails that will be installed in each test module.

Figure 2.8 Canister transfer skid located at an ISFSI used for inserting dry shielded canisters into storage modules with the use of a hydraulic ram.

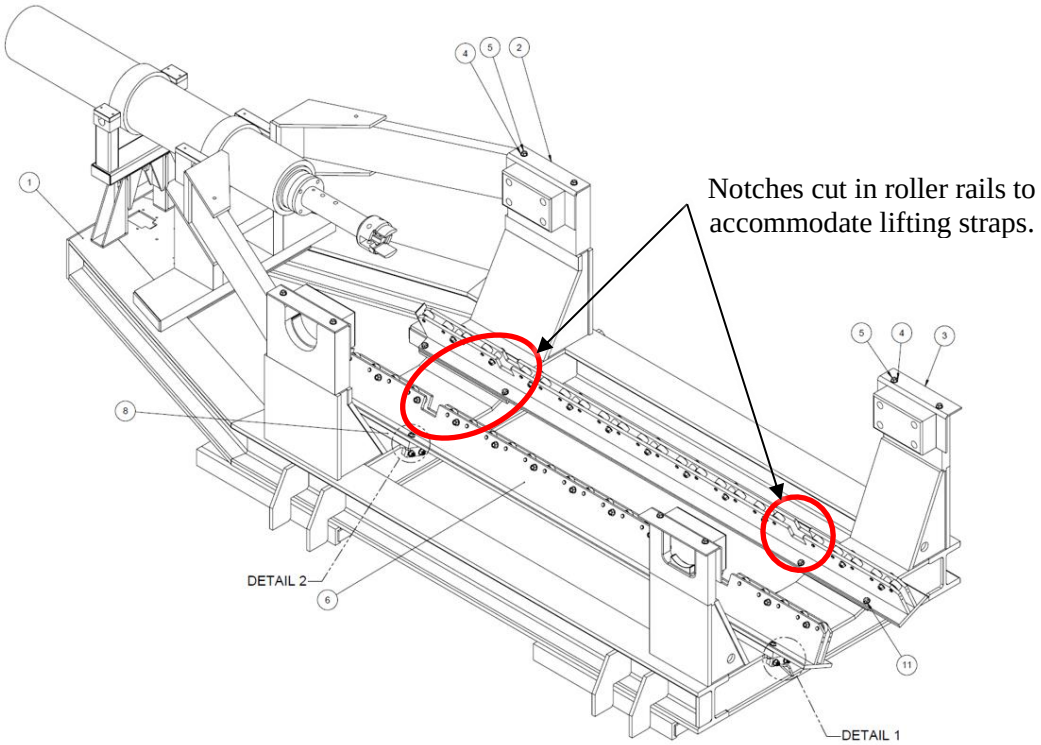

Figure 2.9 Mechanical drawing of canister transfer skid with redesigned roller rails.

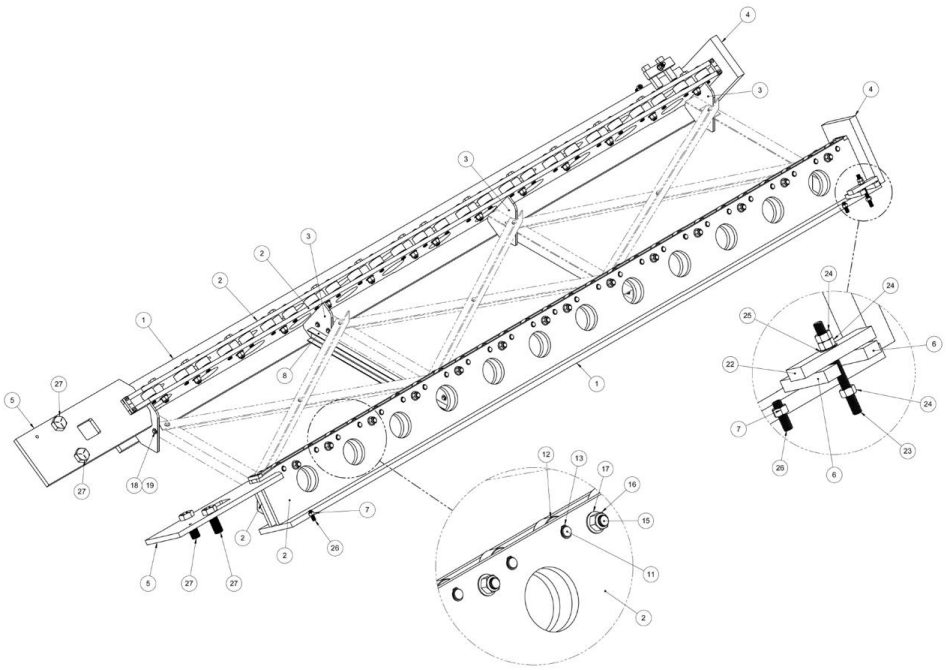

Figure 2.10 Mechanical drawing of roller rails to be installed in the AHSMs.

2.2.2 Thermal Insulation Plan for AHSMs

Modifications will be made to the three otherwise prototypic AHSMs to improve the quality of boundary conditions for model validation and accessibility of the test components. Figure 2.11 shows a rear view of the row of testing AHSMs. The rear access hatch, outlet vents and side and rear insulation (red) are clearly depicted in this view. The exterior insulation provides a near-adiabatic boundary condition for the system, which simplifies thermal modeling of the AHSMs. Between neighboring DCSSs, thermal breaks will be added in the form of intermediate end (transition) walls and insulation. These thermal breaks prevent a high-powered test from influencing an adjacent lower-powered test. Figure 2.12 shows an exploded top view of the AHSMs, revealing the intermediate insulation.

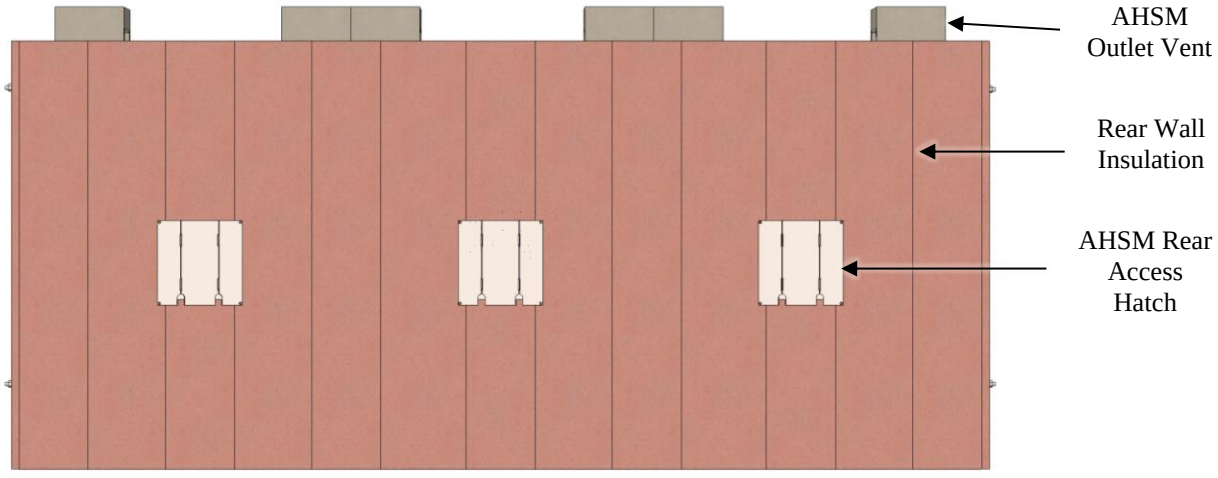

Figure 2.11 Rear view of the test AHSMs.

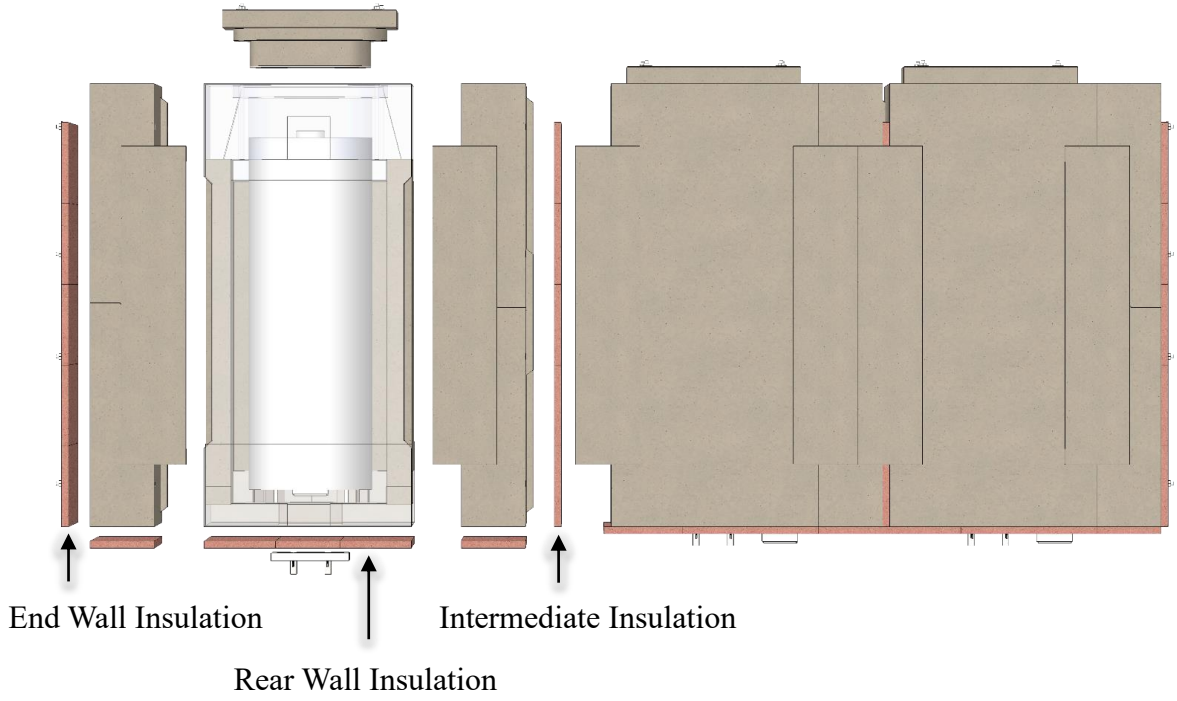

Figure 2.12 Exploded top view of the AHSMs to expose the end wall, rear wall, and intermediate thermal insulation locations.

The AHSM vault door, shown in Figure 2.13, is removeable and provides an opening for the canisters to be loaded and extracted. The front of the AHSMs will not receive any additional insulative layers.

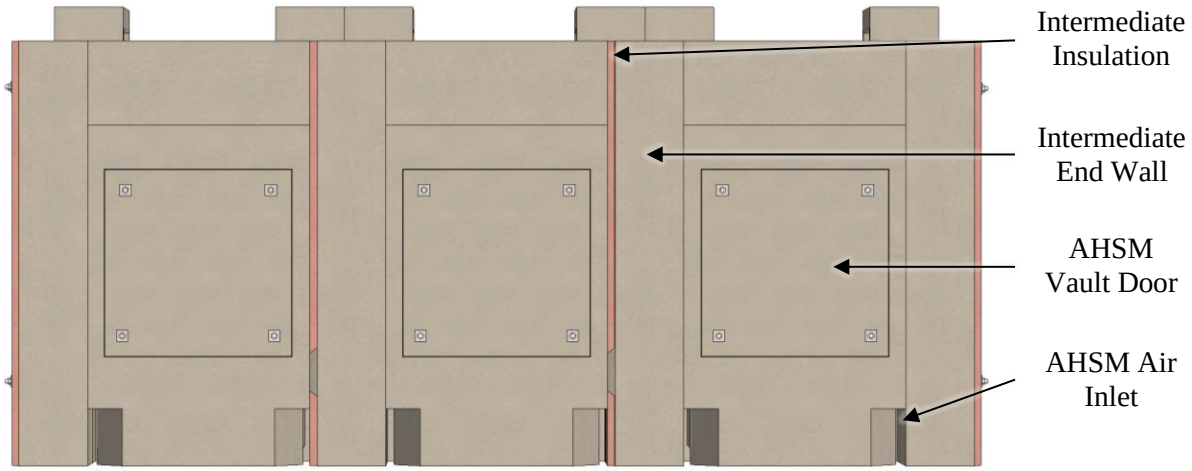

Figure 2.13 Front view of the test AHSMs.

An exploded rear view of the AHSMs is depicted in Figure 2.14. The storage module on the far left of Figure 2.14 has been exploded to reveal the dry shielded canister as it is positioned within the vault. This view also helps to distinguish the various components in the AHSM assembly. The base, front, and rear AHSM walls are exploded for clarity but are an integral unit in reality. The transition walls will be engineered to couple the AHSMs on both sides. Spacers between the AHSMs will be installed to prevent

the compaction of the insulation during coupling. The DSC support rails shown in the exploded rear view of the AHSM will instead be rollers to facilitate insertion and extraction without damaging the canister.

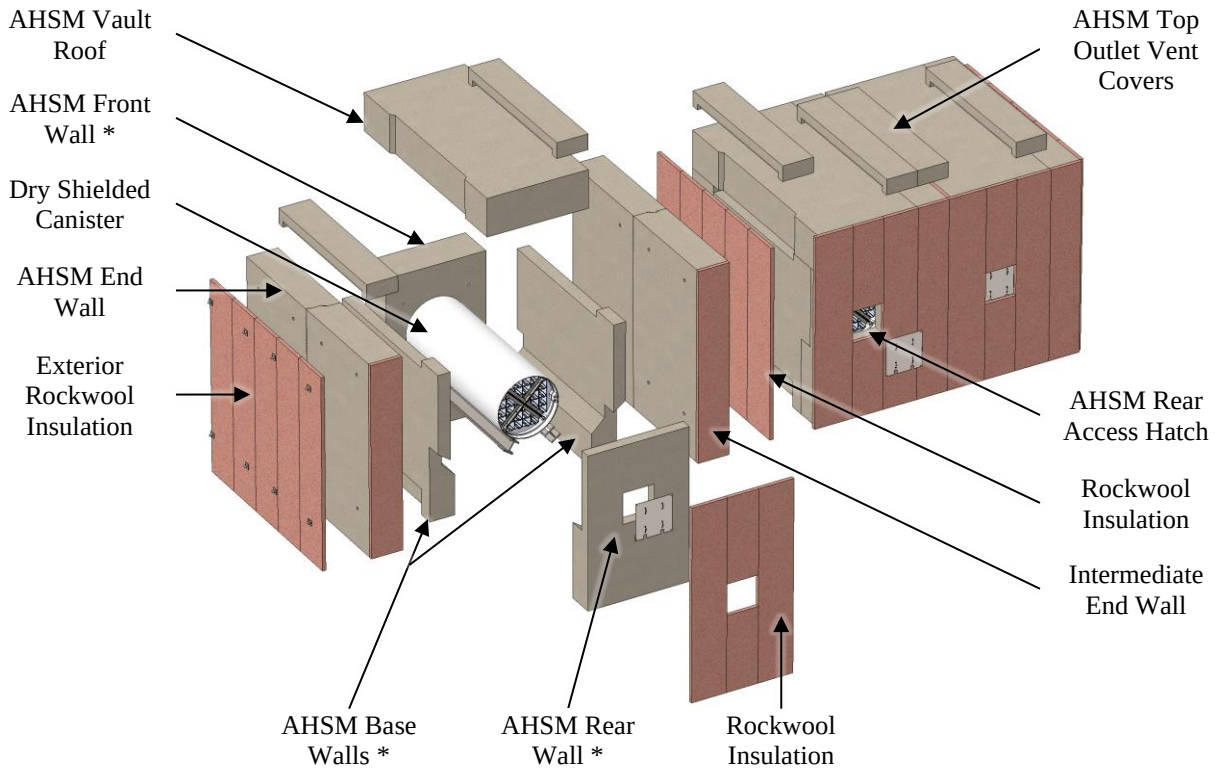

Figure 2.14 Exploded isometric view of an Advanced Horizontal Storage Module, revealing its main components. *Note that the AHSM Base, Rear, and Front walls are shown as exploded components for clarity but are one integral unit.

Previously, a plan to install dividers in the outlet vents was proposed to further limit thermal-hydraulic communication between the different powered DCSSs. Modeling of environmental effects including various wind directions has indicated an increase in the probability of backflow of exhausted air back into the vault system with the inclusion of such dividers, hindering the effectiveness of expelling heat via natural convection. Outlet dividers will not be included in the AHSM assemblies.

2.2.3 AHSM Rear Access Hatch

The concrete AHSM vaults will also be modified to accommodate testing, maintenance, and accessibility of the DSCs. When loaded into the AHSM, the top of the DSC faces the rear AHSM wall. A rear hatch with dimensions of approximately 0.91 × 0.91 m (36 × 36 in.) will be cut in the rear wall of the vault, shown in Figure 2.15, to gain access to power and instrumentation junction boxes recessed into the top of the canister and mounted inside of the AHSM, respectively. The vault hatch will be sealed by the installation of a hatch door as shown in Figure 2.16.

Figure 2.15 Different views of the AHSM showing location of conceptual rear hatch (shown as blue-white checker pattern).

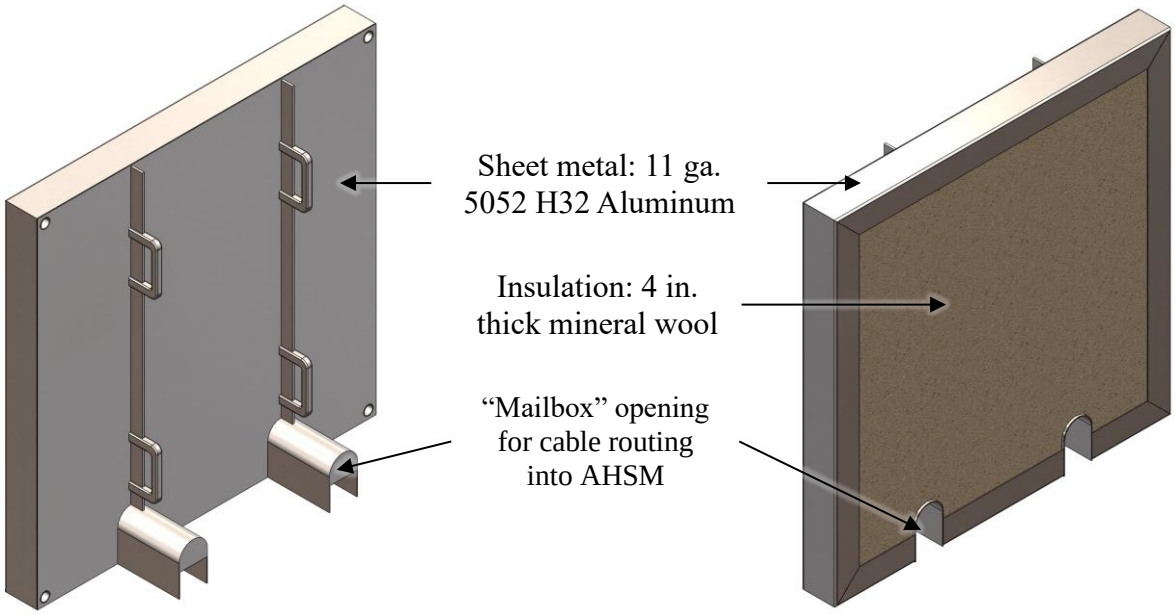

Figure 2.16 AHSM rear access hatch door.

Wiring for the heater power junction box (see red and yellow junction box in Figure 2.17) will exit the vault through the rear hatch access opening. The power junction will be mounted directly to the outer top cover in the recessed space. Temperature-sensitive thermocouple (TC) junctions will be made in a junction box mounted on either a fixture protruding from the outer top cover or to the AHSM rear wall to prevent the box from being in direct contact with the canister (see black and white junction box in Figure 2.17). The components inside of the instrumentation junction box are more temperature-sensitive than the power junction box and cannot be mounted directly to the OTC. In preparation for canister extraction and surface sampling, the connections going from the junction boxes to the data acquisition system and heater power source will be disconnected, as illustrated in Figure 2.18, and the canister should be free of any wiring or connections.

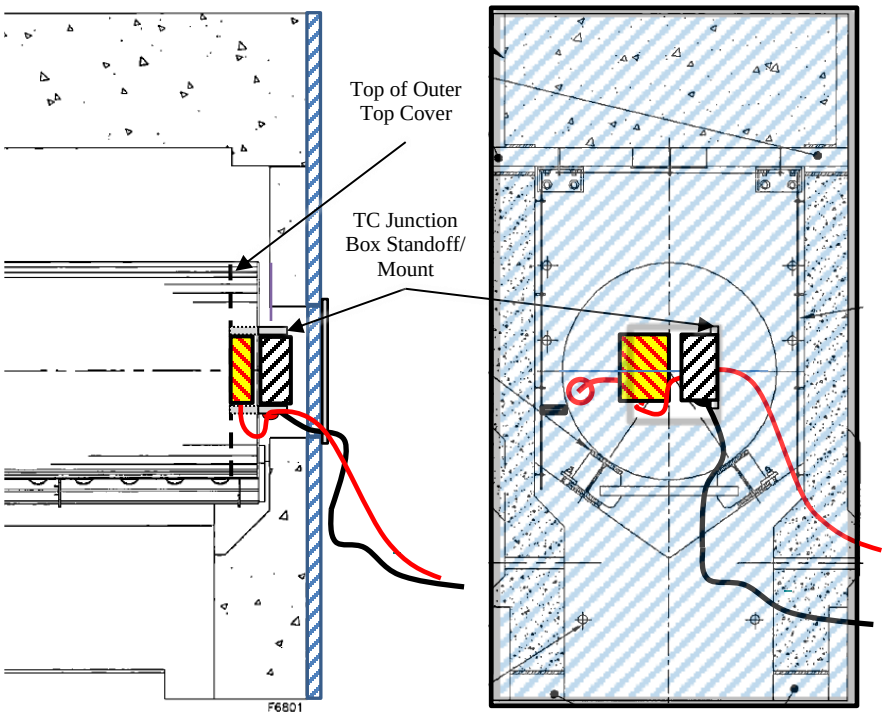

Figure 2.17 AHSM vault modifications (configuration for operations).

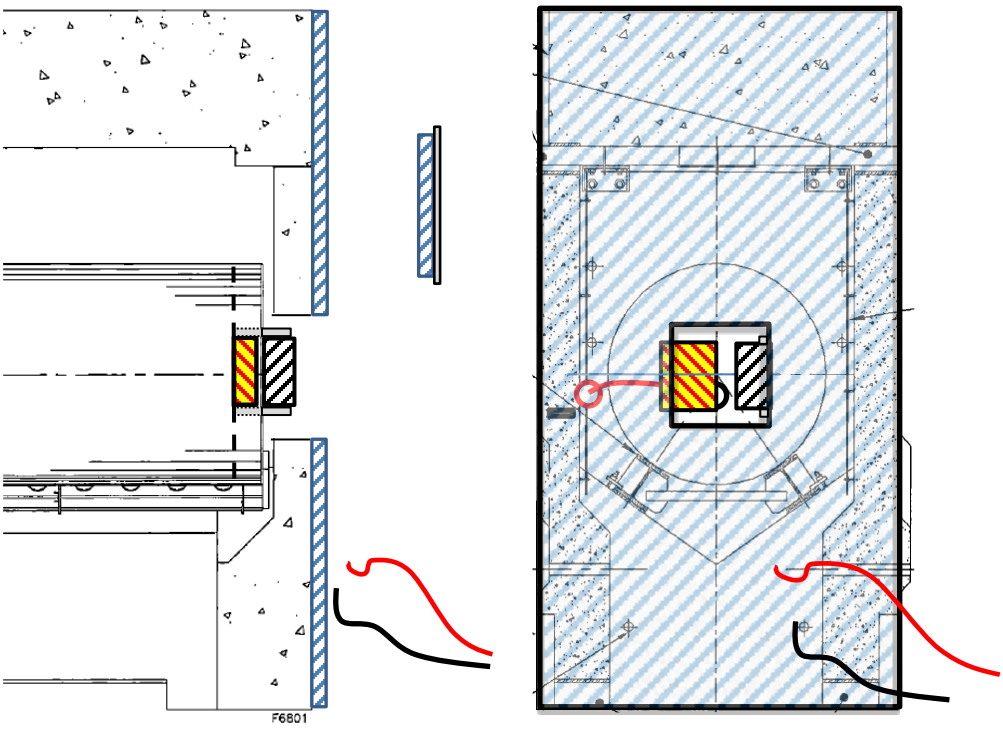

Figure 2.18 AHSM vault modifications (configuration for extraction).

2.3 Component Receipt

Several major components for the CDFD have been manufactured and shipped for storage at the Nuclear Energy Work Complex (NEWC) located inside Sandia National Laboratories in Albuquerque, NM. The largest of these components are the side wall forms as shown in Figure 2.19 and Figure 2.20. The side wall key forms are not shown in the images but are also stored at the NEWC.

Next shown are the roller rails for the AHSM and transfer skid. Figure 2.21 shows the transfer skid rails upon arrival. Figure 2.22 gives two photographs of the roller rails in covered storage at the NEWC. Finally, two photographs of the hatch covers are shown in Figure 2.23. Other various hardware components, such as the transfer skid wedges and mechanical fasteners, are stored separately at the NEWC.

Figure 2.19 Unloading of the AHSM side wall form.

Figure 2.20 AHSM side wall form stored at the NEWC in SNL.

Figure 2.21 Arrival of the transfer skid roller rails.

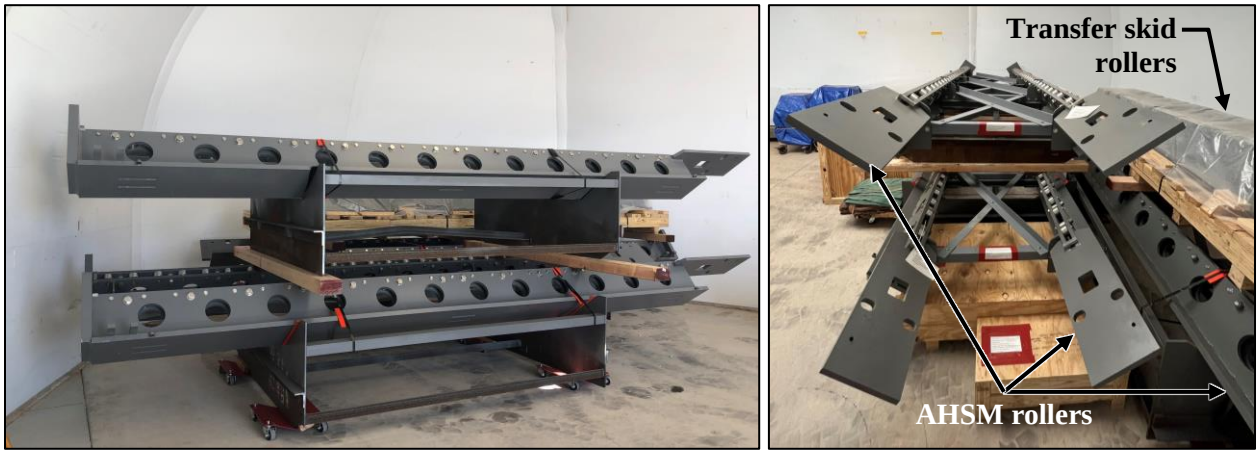

Figure 2.22 Storage of the AHSM and transfer skid roller rails at the NEWC in SNL.

Figure 2.23 AHSM rear hatch covers after unpacking (left) and a standing view (right).

2.4 Instrumentation Plan

Each canister will be instrumented similarly, regardless of the respective applied heat load. Type-K TCs will be installed on each heater assembly inside of the canister. Type-T TCs will monitor the exterior surface temperature of the canister and correspond to surface sampling locations of interest.

2.4.1 Sample Grids

As described in detail in Bryan *et al.*, 2021, the area around each TC location on the exterior of the canister will be sampled on a periodic basis for surface deposits in a regular pattern as depicted in Figure 2.24. Each of the four colored squares represents a sampling location approximately 7.5 × 7.5 cm (3.0 × 3.0 in.) and two types of samples will be collected at each location – a dry sample and a wet sample during every sampling event (see Bryan *et al.*, 2021 for details). Three TCs for each sampling grid will be installed on the exterior surface of the canister. These TCs, indicated by the purple circles in Figure 2.24, are located in the center and opposing corners of the grid to capture the temperature gradient across the sampling windows. Baseline thermal modeling indicates that a maximum temperature difference of 10 °C can exist between the extremes (corners) of the sample windows.

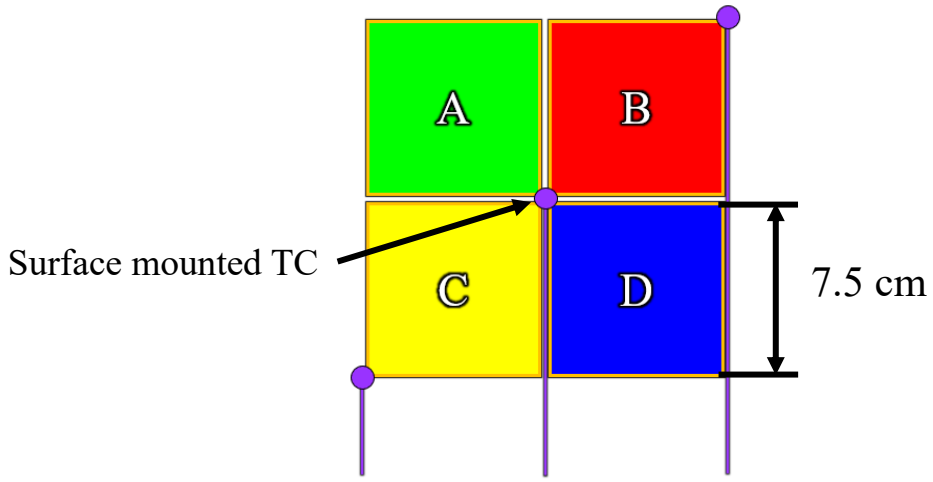

Figure 2.24 Surface deposition sampling pattern.

A possible sampling schedule for each location is summarized in Figure 2.25 [Bryan *et al.*, March 2021] and was constructed to maximize the ability to collect cumulative undisturbed salt deposition and deposition rates over smaller intervals. The four sibling locations around the TC should provide comparable results due to close proximity. Specifically, at each sampling location on the canister, the first grid block (A) will be sampled during the first sampling campaign, one year into the test. During the second sampling campaign, grid block B will be sampled for the first time, and grid block A will be resampled. During each sampling campaign, a new grid block will be sampled, and some subset of the already sampled blocks will be resampled. Each newly sampled block provides cumulative dust and salt load information; resampled blocks provide yearly data [Bryan *et al.*, March 2021].

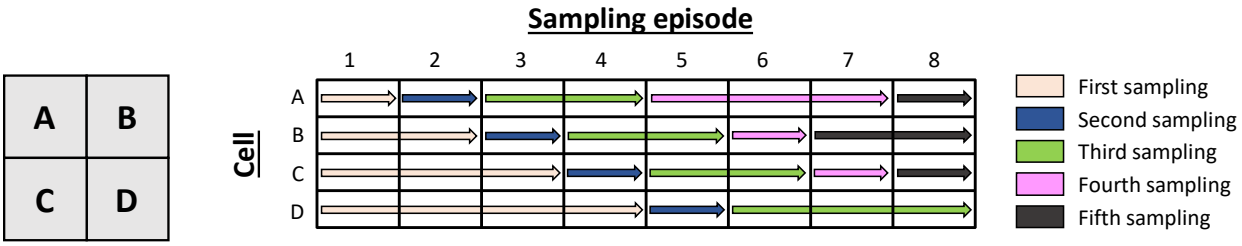

Figure 2.25 Sampling grid and possible sampling schedule [Bryan *et al.*, 2021].

2.4.1.1 Canister Sampling Layout

Sampling locations have been chosen to cover a wide range of different parameters that are anticipated to affect salt and dust deposition on the canister surface [Bryan *et al.*, March 2021]. These parameters include, but are not limited to, canister surface orientation, surface roughness, and fabrication features (e.g., weld seams). Figure 2.26 presents a rendering of a canister and the 20 initially proposed sampling locations. For each of the five longitudinal positions (U through Y), four circumferential locations (1 through 4) will be sampled, except for locations Y3 and Y4, which were deemed inaccessible after further evaluation. Y3 and Y4, shown in red in Figure 2.26, cannot be accessed when the canister is on the transfer skid. The longitudinal locations are equally spaced along the length of the canister. The spacing between sampling grids is approximately 0.91 m (36 in.).

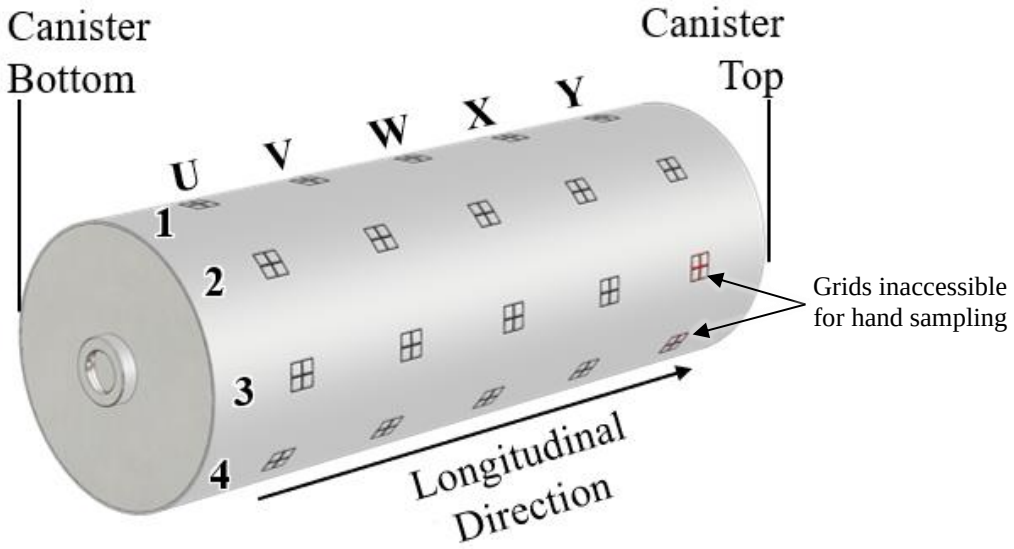

Figure 2.26 Rendering of a dry shielded canister with the proposed surface sampling layout.

2.4.2 External Thermocouples

The exterior surface of the canister will be instrumented with type-T TCs to provide three temperature measurements for each surface sample location as shown in Figure 2.27. Four TCs will also monitor the temperatures of both the canister bottom (shown in Figure 2.27) and the OTC (not shown in Figure 2.27). Type-T TCs were chosen for the exterior instrumentation, given their superior accuracy and stability at ambient temperatures up to around 300 °C compared to type-K thermocouples. Type-T TCs have an accuracy of about ± 1.0 °C or ± 0.75%, whichever is greater. Type-K TCs have an accuracy of ± 2.2 °C or ± 0.75%, whichever is greater. The peak shell temperature for the 40 kW test is expected to be around 240 °C.

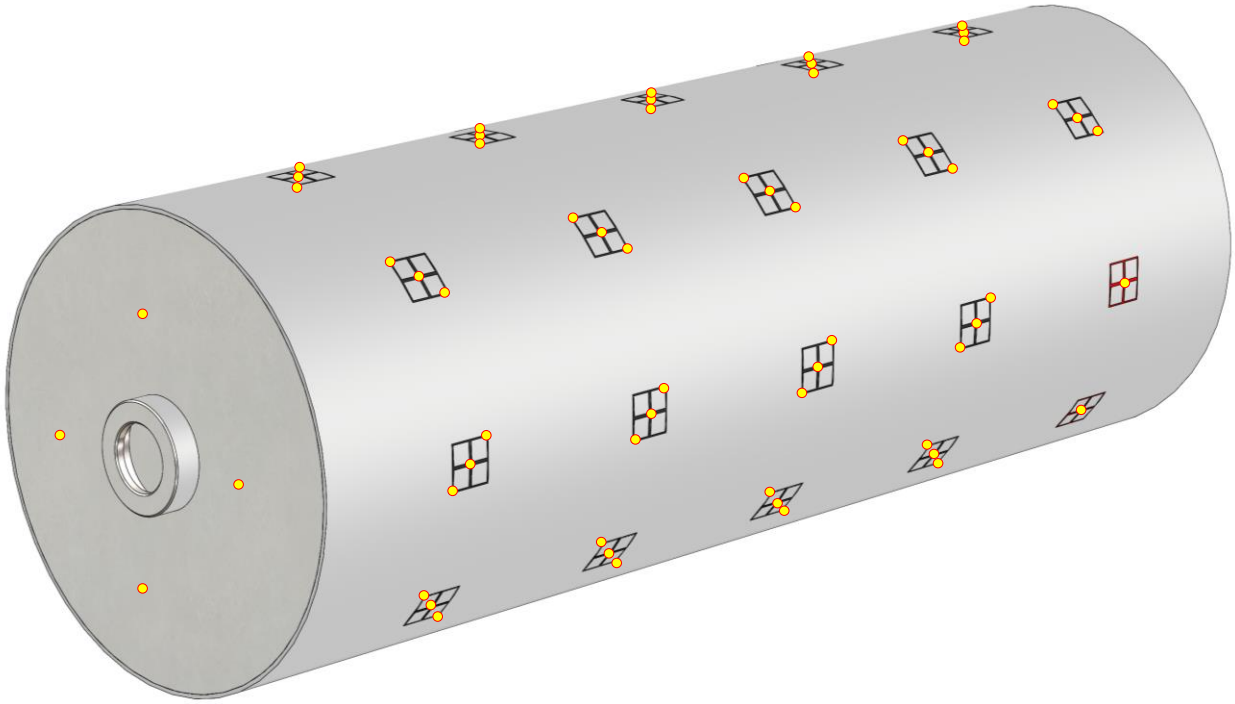

Figure 2.27 External thermocouple layout on canister surface. TC locations indicated by the yellow circles.

An equally important consideration is to make these temperature measurements in a manner that minimizes any flow disturbance of the naturally induced air flow over the canister surface carrying the particulates of interest. To minimize air flow disturbance on the surface of the canister, smaller type-T TCs with a diameter of 0.81 mm (0.032 in.) will be used, and the sheaths will be routed via a TC chase just above the canister support rails as shown in Figure 2.28. The TCs will run straight longitudinally along the canister shell and then route perpendicularly along an arc to the location of interest, indicated by the purple arrow in Figure 2.28. The TC wires will be routed out of the heated zone to the instrumentation junction box located near the rear hatch in the AHSM. If any TCs are installed below the canister support rails, the traverse to the junction box at the back of the vault will be just below the support rail. Because the canister support rails already introduce a significant flow obstruction, the addition of a TC chase in the wake of the rails should not add any significant disturbances.

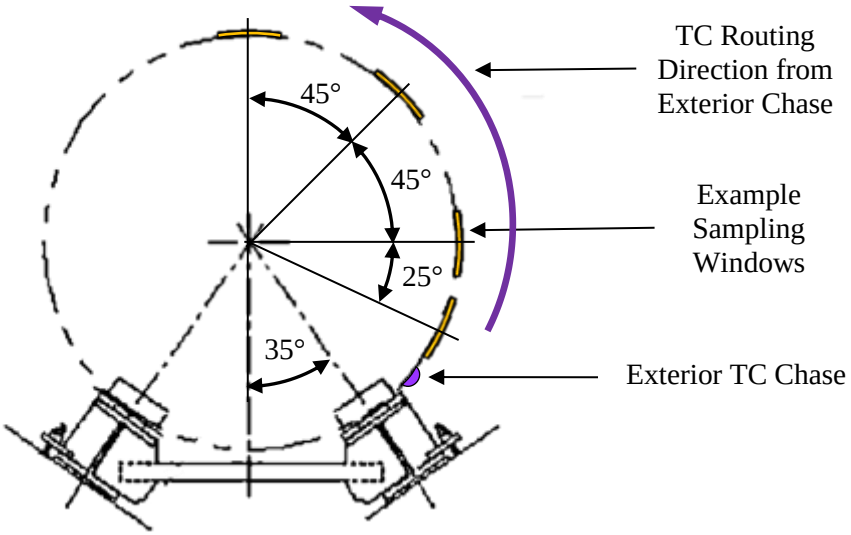

Figure 2.28 End view of a DSC and support rails showing example sampling locations, exterior TC chase, and TC routing direction. Adapted from Figure B.3.1-7 [Transnuclear, 2016].

The TCs on the exterior canister surface will be attached to the DSC shell using SS attachment shims and a resistance welder. The attachment of the exterior TCs must not influence or worsen any corrosion of the canister surface. Enhanced corrosion at a TC attachment point may disrupt the surface deposition composition and potentially lead to TC failure during testing. Previous investigations on the corrosion susceptibility of different TC sheath materials, attachment shim materials, and attachment techniques found that SS TC sheath and shims performed best [Knight *et al.*, 2022].

2.4.3 Internal Thermocouples

The interior of the basket will be instrumented with 1.0 mm (0.040 in.) diameter type-K TCs. Type-K TCs were chosen for the internal thermocouple because of their wider temperature range compared to Type-Ts. The max temperature of a type-K thermocouple is about 1200 °C, compared to about 350 °C for a type-T. The heater assemblies powering the 40 kW canister are expected to reach about 500 °C according to preliminary thermal modeling. Because the internal surface of the basket is largely inaccessible, the internal TCs will be installed on the heater assemblies that are positioned in each of the 32 basket storage cells. Two TCs will be devoted to each heater assembly. One TC will be attached to the heater cladding of each heater within the assembly and exit through the penetrations in the modified outer top cover. The axial locations of interest are shown in Figure 2.29 and listed in Table 2.4. Locations U, V, W, and X align with the locations of the exterior surface sampling grids. Locations B and C represent the extremes of the heated region, where B is located at the U-bend and C is located six inches from the end of the cold pins.

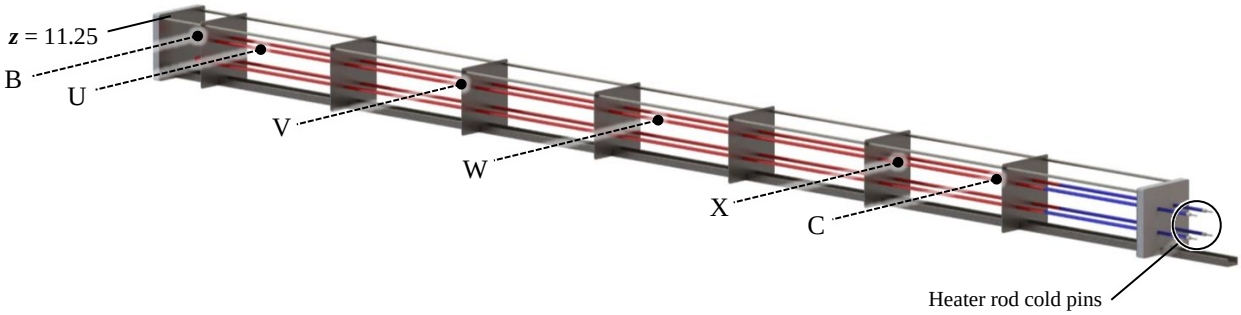

Figure 2.29 Internal thermocouple locations of interest along the length of the heater assemblies.

Table 2.4 Internal thermocouple locations of interest and the corresponding distances from the bottom of the dry shielded canister.

Location Code	Location Description	Distance from Bottom of DSC (z = 0) (in.)
B	Located at the U-bend of the heater	14.25
U	Aligned axially with the “U” sampling region on the canister	27.25
V	Aligned axially with the “V” sampling region on the canister	63
W	Aligned axially with the “W” sampling region on the canister	99.25
X	Aligned axially with the “X” sampling region on the canister	135.25
C	Located six inches from either of the cold pins on the heater	152

Two thermocouples will be installed in each basket cell, one on the top (T) heater, and another on the bottom (B) heater. It is worth noting that the top heater of each cell will be powered with the bottom heater serving as a backup. The limited number of TCs will produce a low-resolution measurement of the thermal profile of the inside of the DSC. The proposed layout for the internal TCs is shown in Figure 2.30 The greatest number of TCs will be installed at the W-location, aligned with the “W” sampling grids on the canister surface. This concentration of TCs at one location will provide a finer-resolution examination of the temperature distribution in a canister cross-section. The remaining TCs are arranged to provide

symmetry checks about a plane of half symmetry running through the centerline of the canister, aligned with gravity. A representation of the symmetry plane is shown by the green dashed line in Figure 2.30.

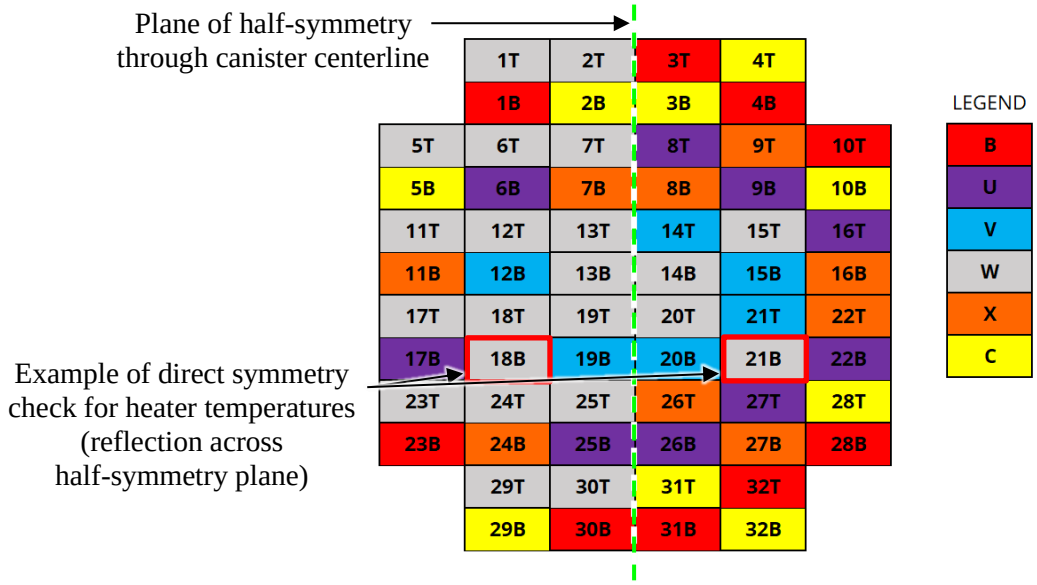

Figure 2.30 Preliminary layout of internal thermocouple locations. Each heater rod will be instrumented with one TC installed at the axial location indicated by the legend and Table 2.4.

2.5 Simulated Field Testing

Transfer skid and AHSM rear wall mockup structures were designed and fabricated at the NEWC in SNL. The transfer skid mockup has and will continue to provide the CDFD sampling team opportunities to identify and rehearse a proper procedure for surface sampling. The AHSM rear wall mockup allows the testing team to gain an understanding of, and experience working with, the limited accessibility of the DSC while inside of the AHSM.

2.5.1 Mockup Structures

2.5.1.1 Canister Standoff

The height from the ground to the centerline of the canister is 2.7 m (8ft. 10in.) during normal testing and sampling operations. A canister standoff was designed and built to provide the sampling and testing teams experience working with a canister at prototypic height. Fabrication of the canister standoff was completed in June 2022. Figure 2.31 shows the canister standoff during fabrication. The transfer skid mockup is constructed from W8 x 48 structural steel H-beams to support the 23,000 kg (50,000 lb.) load of the 32PTH2 canister.

Figure 2.31 Fabrication of canister standoff at the NEWC in SNL.

Figure 2.32 shows a prototypic spent fuel canister being placed on the canister standoff at the NEWC in SNL. Figure 2.33 shows the canister elevated off the ground at the prototypic height when on the transfer skid for sampling or inside the AHSM vault during normal testing operations.

Figure 2.32 Placement of 32PTH2 dry shielded canister onto standoff.

Figure 2.33 32PTH2 dry shielded canister at prototypic height of 8'10" from ground to central axis of the canister.

2.5.1.2 Transfer Skid Mockup

Figure 2.34 shows a rendered drawing of a loaded canister transfer skid and the transfer skid mockup. Once the heaters have been turned off, the canisters will be allowed to cool within their overpacks. The canister will be on the transfer skid during sampling operations. The width of the transfer skid, which is significantly wider than the canister, will restrict approach to the lower parts of the canister. The trunnion posts, indicated by the red boxes in Figure 2.34, are an example of features on the transfer skid causing limitations on accessibility during surface sampling. The gap between the trunnion posts is about 0.3 m (11 in.). Finally, the canister will not be extracted completely from the AHSM overpack, and the approach to the canister with machinery will be restricted by the proximity to the overpack. These obstructions have been faithfully included in the mockup to provide a realistic setting for the sampling team to rehearse and develop their sampling procedures.

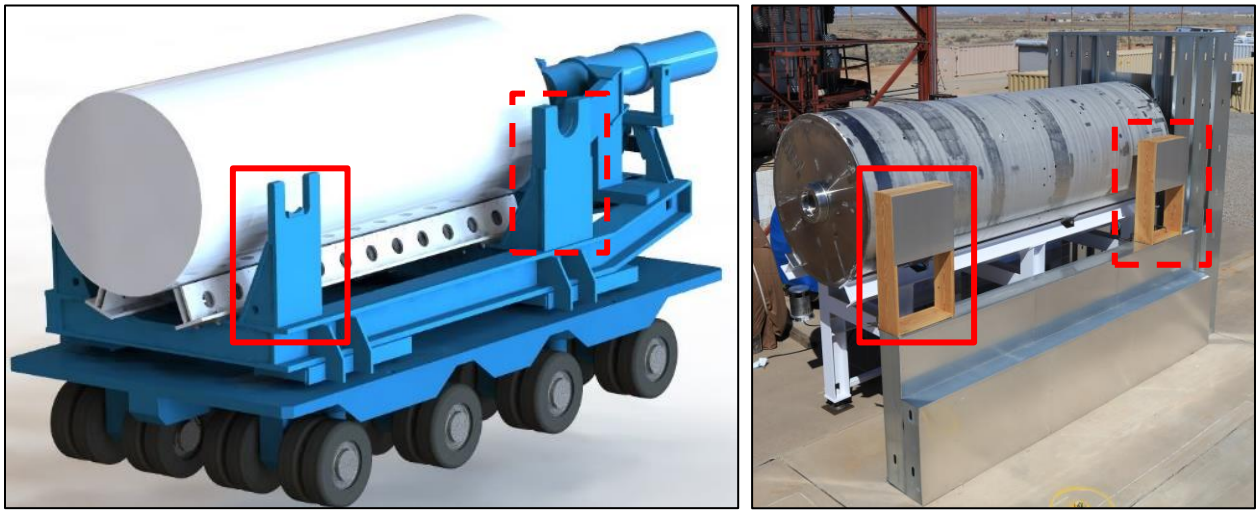

Figure 2.34 Computer-aided design of the canister transfer skid (left) and the transfer skid mockup located at Sandia/New Mexico's Surtsey site (right). The trunnion posts in each image are indicated with red boxes.

2.5.1.3 AHSM Rear Wall Mockup

An AHSM rear wall mockup has been built around the canister standoff and is shown in Figure 2.35. The AHSM rear wall mockup will allow the testing team to experience the accessibility of the DSC through the access hatch while it is loaded in the vault. This allows familiarity with the confined opening and limited accessibility to the power and instrumentation junction boxes. The best practice for cable routing and management will also be determined with the use of the mockup wall.

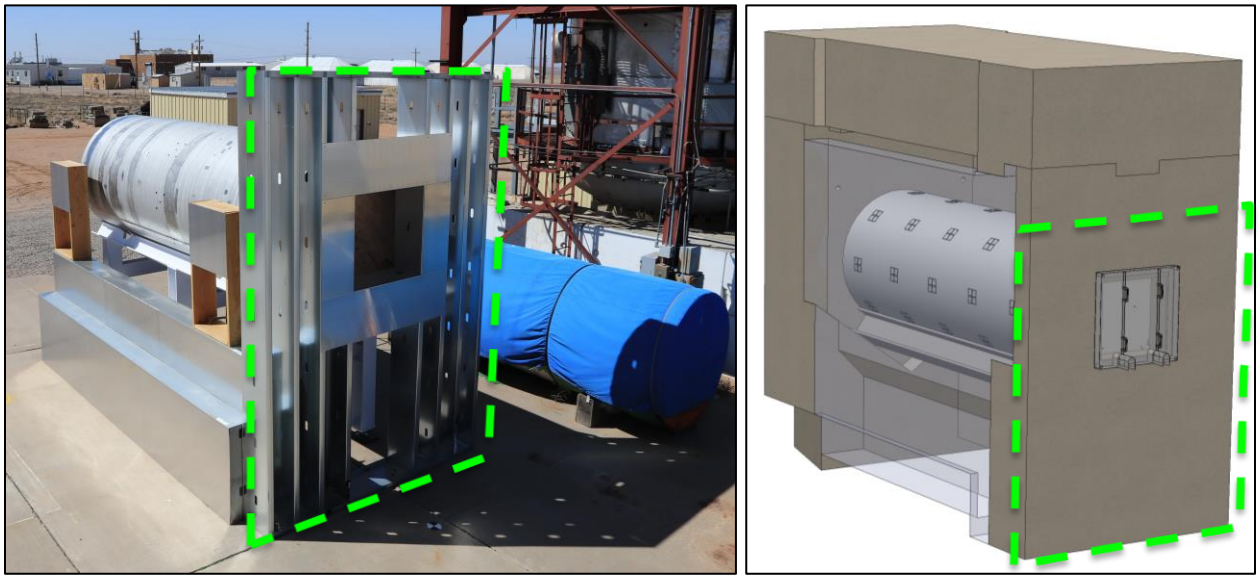

Figure 2.35 AHSM rear wall mockup located at Sandia/New Mexico's Surtsey site (left) and rear view of single AHSM (right).

2.5.2 Manual Sampling Episode

A staged field test for manual sampling of a canister took place at the NEWC in SNL. The procedures and results of the staged field test are discussed in detail in Knight *et al.*, 2023. For safety, personnel will not be allowed to climb onto the skid for surface sampling; access to the canister surface will employ a boom lift or similar device. Sampling locations of interest, as described in Section 2.4.1.1, were first assessed with an articulated boom lift. This activity evaluated the accessibility of the proposed sampling locations and provided an opportunity to discuss and practice the sampling procedure. Sampling plates with known quantities of salt deposits were then mounted to the canister surface and the salts were collected off the plates using a sampling template and sponges. A drawing of a sampling plate and template is shown in Figure 2.36. This purpose of this activity was to establish a proper sampling procedure, familiarize the sampling team with the equipment that will be used in the field, and evaluate the efficiency of the sampling method. Pictures from the staged field testing are shown in Figure 2.37.

Figure 2.36 Drawing of the mock sampling plate and sampling template used for the simulated field testing.

Figure 2.37 Practice surface sampling was conducted at the NEWC in SNL.

2.5.3 Rehearsal of Canister Insertion and Extraction

The bottom edge of the rear access hatch is about 2.2 m (7ft. 4in.) from the ground. Rolling stairs, shown in Figure 2.38, will be used to gain access to the rear access hatch and perform work on the canister inside of the AHSM. Figure 2.39 demonstrates the accessibility into the AHSM via the rear access hatch. The AHSM rear wall mockup will become ever-more valuable for establishing a procedure for providing power and connecting instrumentation to the canister and prepping the canister for extraction during hand sampling episodes.

Figure 2.38 Rolling stairs positioned in front of the AHSM rear wall mockup.

Figure 2.39 Member of the testing team evaluating the accessibility of the canister through the rear access hatch of the AHSM.

The testing team attempted a dry fit of the rear access hatch cover, shown in Figure 2.40. Rehearsal prior to canister and test deployment ensures the components used can be handled and installed safely. The hatch cover dry fit assured the team that the rolling stairs are at a comfortable height and width for two members to work.

Figure 2.40 Dry fit of the rear access hatch cover.

2.6 Atmospheric Monitoring

Ambient monitoring will be conducted at or near the ambient air inlets of the storage vaults. Continuous monitoring will include typical weather station parameters such as air temperature, absolute ambient pressure, wind speed and direction, humidity, and precipitation. Additionally, particulate matter sensors will be used to continuously monitor various size ranges of aerosols in the air. Deposition models require the particle composition and density (mass per m^3 air), as well as size distribution, for inputs. Periodically, on-site aerosol sampling will be conducted to characterize these parameters.

2.6.1 Weather Station

The ATMOS 41 all-in-one weather station from METER Group has been chosen for collecting meteorological data at the test site. The weather station and accompanying data logger are shown in Figure 2.41. This weather station measures precipitation, relative humidity, air temperature and pressure, and wind speed and direction.

Figure 2.41 ATMOS 41 all-in-one weather station and accompanying ZL6 data logger to be used at the host site for atmospheric monitoring.

2.6.2 Ambient Aerosol Characterization

A cascade impactor provides real-time particle size data and retains the samples for later chemical composition analysis [Bryan *et al.*, September 2021]. This analysis informs composition of the particles as a function of particle size. Cascade impactors consist of a series of stages, each of which captures progressively smaller aerosol particles from an airstream passing through it. This allows a particle size distribution to be determined. For the CDFD, an impactor is required that is suitable for outdoor environmental monitoring, that retains the samples for later chemical analysis, and that can collect material over a significant amount of time, requiring less frequent exchanges of the impactor targets. Equipment from several different manufacturers was evaluated, and an impactor offered by Dekati Ltd. has been chosen. The sampling instrument is shown in Figure 2.42.

Because of particle size limitations, cascade impactors are frequently coupled with other instruments that do particle sizing and particle density measurements. To complement the cascade impactor, a TOPAS LAP 322 Laser Aerosol Particle (LAP) Spectrometer will be used. This aerosol sampling instrument is shown in Figure 2.42. Inlet vents located at the top of each instrument will prevent extremely coarse particles from entering the systems. The inlets nominally have a 15-20 μm opening for the cascade impactor and a 40-50 μm opening for the particle sizer. These instruments will provide valuable data regarding the chemical species in the ambient air at the host site and what could potentially deposit on the canister surface.

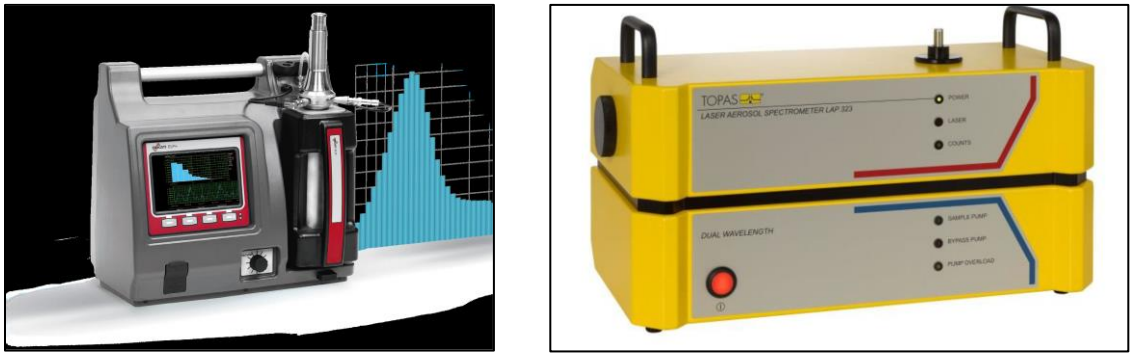

Dekati Cascade Impactor TOPAS Laser Particle Sizer

Figure 2.42 Dekati cascade impactor (left) and TOPAS laser particle sizer (right) for ambient aerosol site characterization.

This page is intentionally left blank.

3 SIMULATED DECAY HEAT

3.1 Power Control

To achieve accurate and controlled heat load settings, the heaters will be powered using Control Concepts MicroFUSION silicon-controlled rectifiers (SCRs). The total power delivered to each circuit will be independently measured using Ohio Semitronics multifunction power meters model APlus, which provide high-accuracy true root mean square measurements for voltage, current, power, and power factor. They are specifically designed to accommodate distorted and chopped waveforms typical of SCRs. Similar power control systems have been used in previous studies with excellent results [Pulido *et al.*, 2022]. Electrical power will be provided by 480V three-phase service. The line-to-neutral voltage of this service is 277V, which will be supplied directly to the SCRs, through the power-monitoring APlus, then to each heater zone.

The data acquisition (DAQ) system will be built for reliability and flexibility. A National Instruments (NI) peripheral component interconnect extensions for instrumentation – express (PXIe) chassis has been chosen given its scalable performance. Power control will be managed through this system using LabVIEW. CompactDAQ (C-DAQ) systems have been chosen for TC measurements as they offer enhanced simplicity given their ethernet communication to the PXIe. Each C-DAQ chassis can accommodate up to 128 TCs with the implementation of eight NI 9213 TC modules, each with enough slots for 16 TCs. Approximately two C-DAQ chassis will be needed for each canister. A total of 128 TCs (64 internal, 64 external) are currently planned for each canister. Additional thermocouples will be installed for ambient measurements inside and outside of the AHSMs and will require an additional chassis, but could be shared amongst each module, depending on the length of the TC wires.

3.2 Preliminary Heater Testing

Preliminary *in situ* heater tests were conducted to check the adequacy of the preliminary U-tube heater design and serve as a benchmark for thermal modeling. Twelve electrical heater assemblies arranged in the "corner-center" configuration are shown in Figure 3.1 which serves as the current heater layout for testing. The basket locations are numbered serially starting in the upper left corner. Each heater is assigned a unique identifier (*e.g.*, "HA" for heater "A"). Uniform power was supplied to each heater assembly for these preliminary tests. The red, blue, and green colors in Figure 3.1 designate the power control circuit used (circuits A, B, and C). Cladding on two of the four heaters in the center of the basket assembly (HK and HM) were painted with a high-emissivity coating of known emissivity of 0.9. The coating did not survive testing and heater cladding will remain uncoated for the test. In comparison, the emissivity of the pre-oxidized cladding is about 0.5.

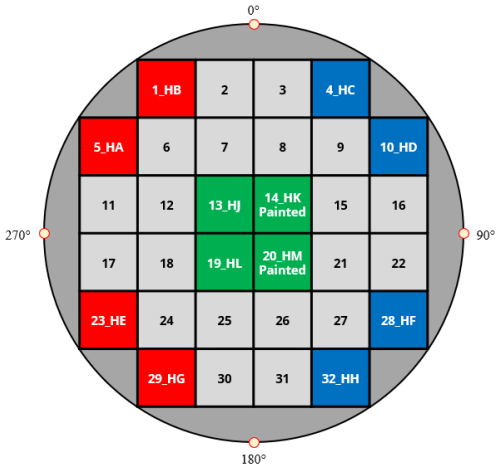

Figure 3.1 12-heater "corner-center" configuration for CDFD preliminary heater testing.

3.2.1 Preliminary Heater Design

The goalpost radiative style heater design shown in Figure 3.2 has been used for preliminary testing. The U-tube heater is centered on a SS316 C-channel backbone. Thermal radiation shields are located on each end of the heater assembly and produce more prototypic canister skin temperature profiles. This design provides near-symmetric heat transfer into the fuel compartment.

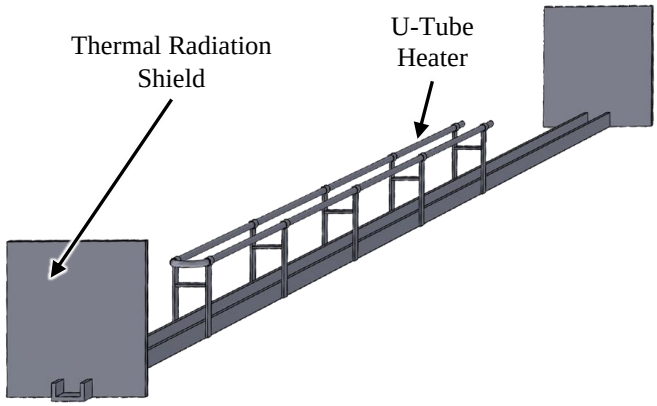

Figure 3.2 Goalpost radiative heater design with thermal radiation shields on both ends.

3.2.2 Preliminary Heater Test Results

Preliminary heater tests have been run at total applied heat loads ranging from 4.8 to 35.0 kW. Table 3.1 presents the steady state maximum temperatures for the heater assemblies and canister shell for each heat load tested. The locations of the TCs which recorded the maximum shell temperatures are also listed in Table 3.1. The max temperature on the canister surface was consistently located on the canister belly (depicted as 180° in Figure 3.1), approximately 2.2 m (85 in.) from the bottom end of the canister. Peak heater and shell temperatures are plotted against total applied heat load in Figure 3.3. Peak canister shell temperature increased approximately linearly with respect to heat load.

Table 3.1 Steady state peak heater and shell temperatures are listed for each heat load tested.

Total Heat Load (kW)	Peak Heater Temperature (°C)	Peak Shell Temperature (°C)	Location of Max for Peak Shell Temperature
4.8	226	61	$\theta = 180°$, $z = 3.6$ m
9.6	339	85	$\theta = 180°$, $z = 2.2$ m
12.0	386	97	$\theta = 180°$, $z = 2.2$ m
14.4	426	112	$\theta = 180°$, $z = 2.2$ m
20.0	494	131	$\theta = 180°$, $z = 2.2$ m
25.0	551	156	$\theta = 180°$, $z = 2.2$ m
30.0	598	177	$\theta = 180°$, $z = 2.2$ m
35.0	633	196	$\theta = 180°$, $z = 2.2$ m

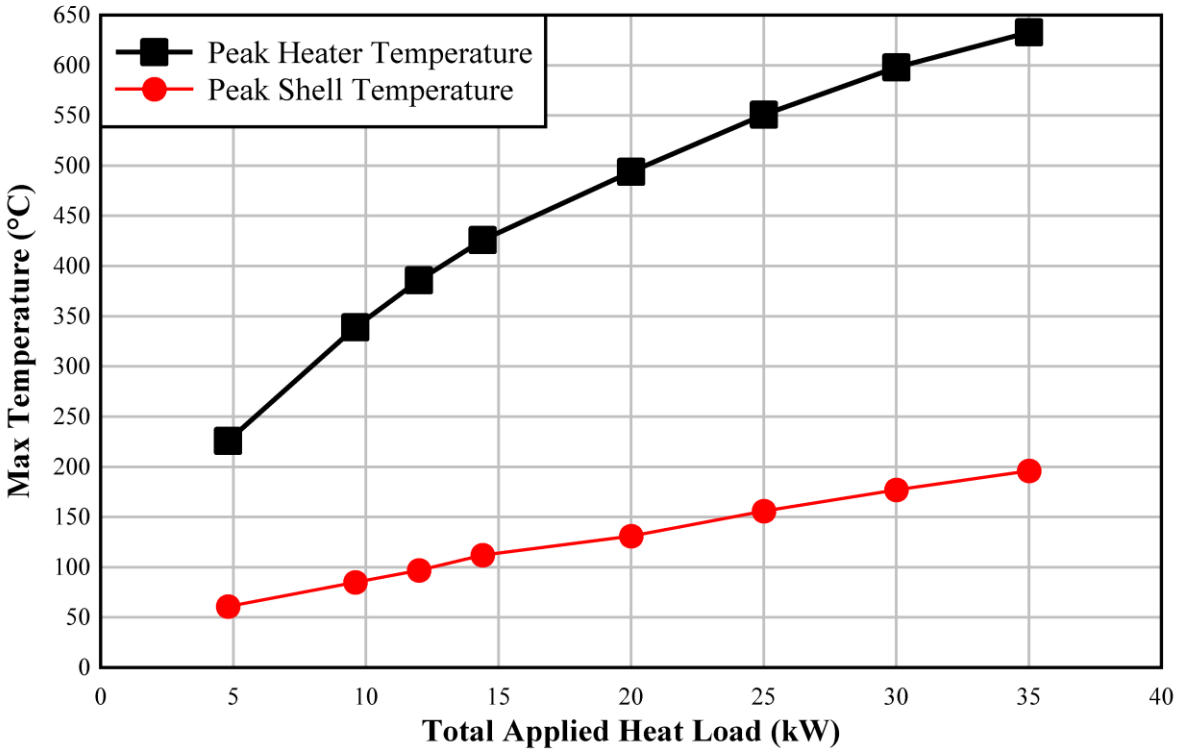

Figure 3.3 Peak heater and shell temperatures plotted against total applied heat load.

The transient heater temperatures and surface temperatures at the four cardinal coordinates for a test at 35.0 kW are presented in Figure 3.4. The hottest shell temperatures at the cardinal coordinates occurred roughly 2.2 m (85 in.) from the bottom end of the canister. The peak heater temperature was located 85 in. away from the bottom end of the canister on heater HJ in basket cell 13.

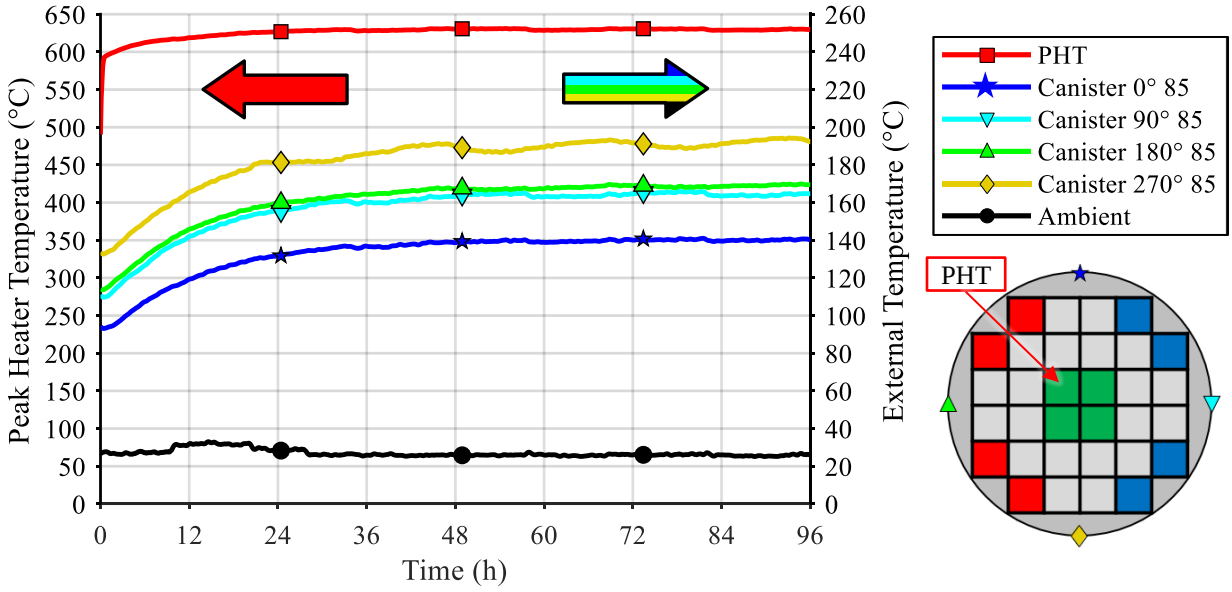

Figure 3.4 Transient peak heater temperature (PHT) and canister surface temperatures measured with 35.0 kW total applied power to the 12-heater "corner-center" configuration.

Among all tests run to date, the highest surface temperature is at the circumferential bottom of the canister (180°) and the coolest is located at the top of the canister (0°), as would be expected. The basket assembly is nonconcentric with the DSC shell. The basket assembly, bottom aluminum support rails, and canister shell make intimate contact, increasing the heat transfer from the basket assembly to the shell exterior through conduction rather than purely radiation. The temperatures on the sides (90° and 270°) are similar, indicating symmetry among the left and right sides of the canister. Due to the thermal mass of the canister, it took at least four days to reach steady state. Note that the boundary conditions for these preliminary tests represent natural convection into an open room, which differs significantly from the confined natural convection boundary conditions found inside the AHSM. Figure 3.5 shows thermal images of the canister internals and exterior surface during a 20.0 kW test.

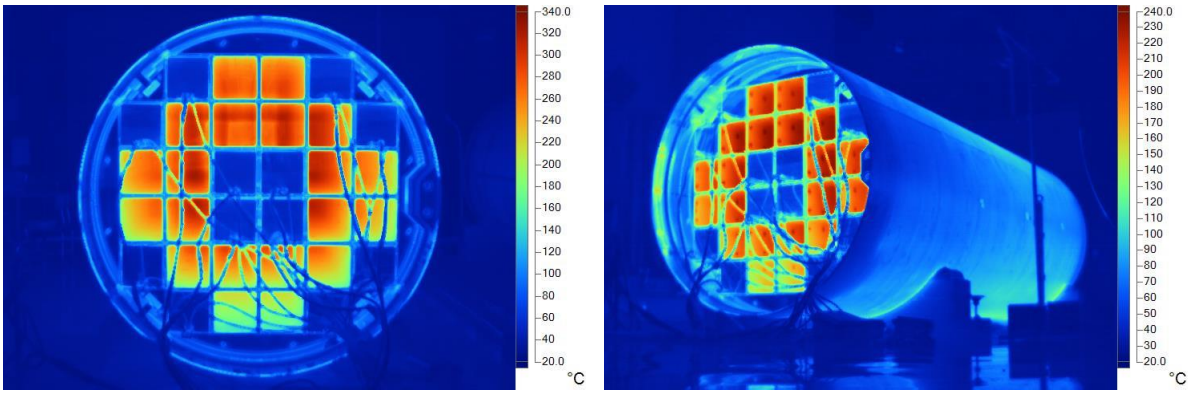

Figure 3.5 Thermal images taken with an infrared camera during a 20.0 kW test. The thermal radiation shield was removed to expose the canister internals.

3.2.3 Canister Shell and Basket Gap Measurements

Typically, after the drying procedure is finished and the dryness criteria is satisfied, the DSC is backfilled with helium gas to an internal pressure of about 800 kPa (8 bar). The CDFD canisters will not be pressurized or backfilled with an inert gas. The thermal conductivity of helium is about five to six times greater than that of air for the temperatures of interest (ambient up to 500°C). The heat transfer from the heater assemblies to the canister shell is significantly impacted by the gaps between the basket and shell. To characterize the gaps around the circumference of the canister opening, steady state measurements were taken at each heat load. Figure 3.6 shows canister gaps being measured with a wedge gauge while the canister was at ambient temperatures and unpowered. Canister gaps were also measured with a wedge gauge while the can was at steady state when powered. Proper personal protective equipment was donned while taking gap measurements for the higher-powered tests.

Figure 3.6 Canister-basket gap measurements taken with a wedge gauge at the 300° location on the canister while at ambient temperatures.

The canister gap measurements are an important factor for an accurate thermal model of the CDFD test system, especially because of the lack of helium backfill to promote heat transfer to the canister shell. As temperature increases, the basket assembly expands inside and gaps between the basket and canister shell shrink. Figure 3.7 shows a graphical representation of the gaps at each radial location measured for tests ranging from unpowered (ambient) up to 35.0 kW. Gaps were measured at each of the marked angles in Figure 3.7. The lines connecting the measurements are simply the linear transitions between points. The canister gap is largest, and easiest to visualize in Figure 3.7, at the top (0°) of the canister. At the top of the canister, the gap shrinks from about 6.9 mm (0.27 in.) to 3.6 mm (0.14 in.). This change is likely a combination of thermal expansion of the basket and the canister shell softening and further deforming from its own weight, deviating from a noncircular opening. Due to the vent and siphon block, gap measurements were inaccessible at 90° and were instead taken at 77° and 103°.

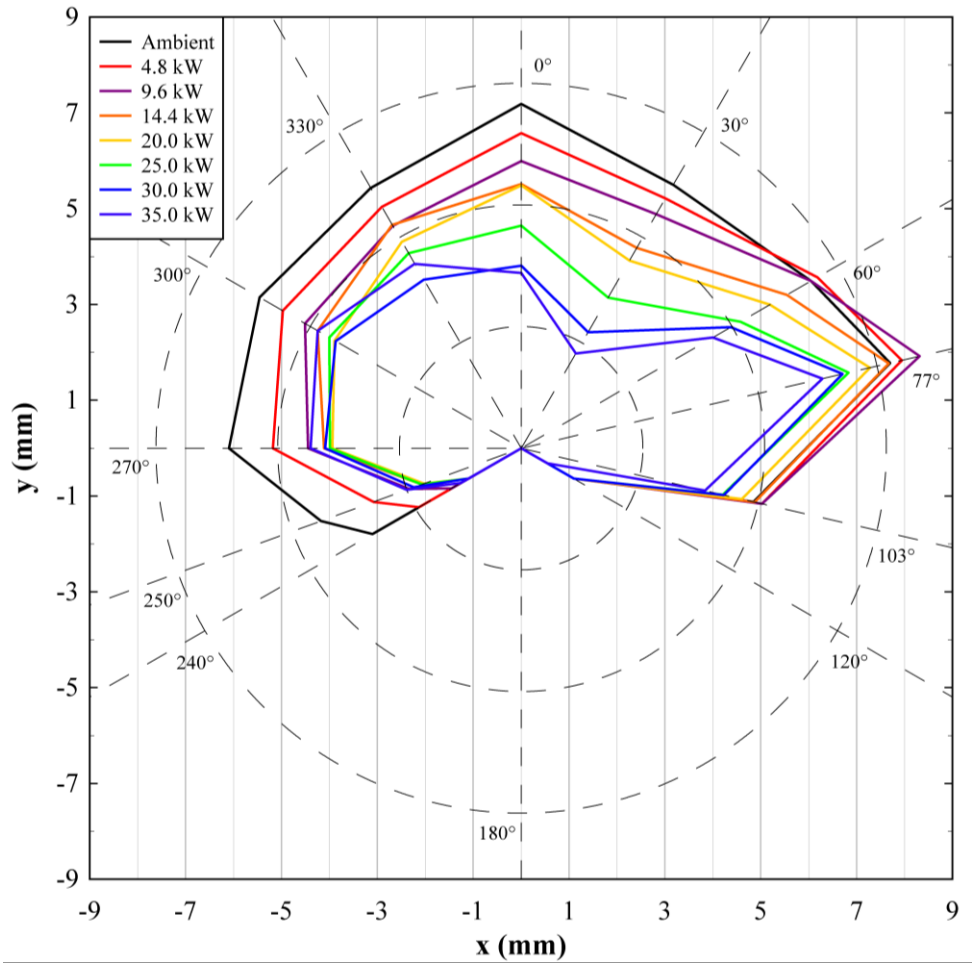

Figure 3.7 Canister-basket gap measurements for ambient temperatures up to 35.0 kW

3.3 Final Electrical Heater Design

Preliminary heater tests indicated that U-tube heaters are appropriate surrogates for SNF and can adequately heat the DSC. The final heater assemblies are designed for durability and longevity. The heater assembly, shown in Figure 3.8, features two U-tube heaters, providing longevity of the assembly through redundancy. One heater will be run at a time with the other as a backup in the case of heater failure. As shown in Figure 3.8, the U-tube heaters have a heated region 3.65 m (144 in.) in length and feature a 0.58 m (23 in.) long cold pin on both ends. The cold pins were extended past the insulation to facilitate power connections. The SS316 U-channel positions the heater assembly so that the center of the heated region aligns with the prototypical center of the SNF heated region, 1.9 m (76 in.) from the interior of the bottom shield plug. The U-channel also serves as a TC chase for the thermocouple wires to be routed to the top end of the canister.

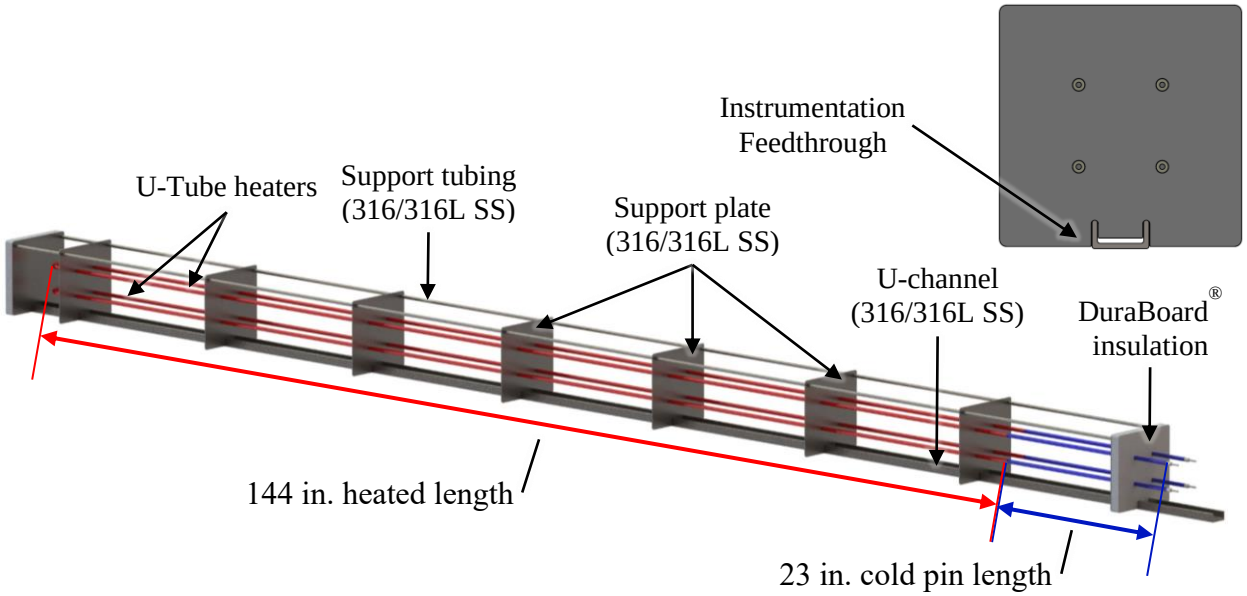

Figure 3.8 Final heater assembly design.

Figure 3.9 shows an as-built heater assembly. Heater cladding is Incoloy 800 and was pre-oxidized during fabrication to limit the oxidation buildup and changes in emissivity throughout the life of the heater. All support material including the support plates, support tubing, and U-channel backbone is dual-certification SS316. Thermal insulation boards nominally 2.5 cm (1 in.) thick are located at each end of the heater assembly to prevent heat loss through the bottom shield plug and outer top cover of the canister.

Figure 3.9 As-built final heater assembly.

3.3.1 Heater Profile Development

Four of the final heater assemblies were instrumented with thermocouples and installed into basket cells 13, 14, 19, and 20, depicted by the diagram in Figure 3.10. The heater assembly in cell 13 was instrumented with 25 TCs along the heated length to develop a detailed thermal profile of the tube heater. Each of the heater assemblies in cells 14, 19, and 20 were instrumented with three TCs along the heated length to evaluate the symmetry in neighboring basket cells and the performance of the other heaters in relation to the more densely instrumented heater in cell 13. Figure 3.10 presents steady state temperature data for heaters in cells 13 and 14, each powered at 1.67 kW (20.0 kW total heat load for the 12 heaters), plotted against the distance from the canister bottom. The solid symbols represent TCs installed on the left side of the U-tube heater and the open symbols represent TCs located on the right.

The max temperature of heater 13 was 437 °C located about 2.0 m (79 in.) from the canister bottom. The minimum temperature of heater 13 was 401 °C and occurred at the U-bend of the heater, about 0.3 m (13 in.) from the bottom of the canister. Heater 14 followed the same trend of heater 13 with the maximum temperature near the middle of the heated region. The temperature closely matched heater 13 as well. All values for corresponding locations between heaters 13 and 14 fell within about ± 2% (± 7.5 °C), close to the uncertainty of type-K thermocouples at these temperatures.

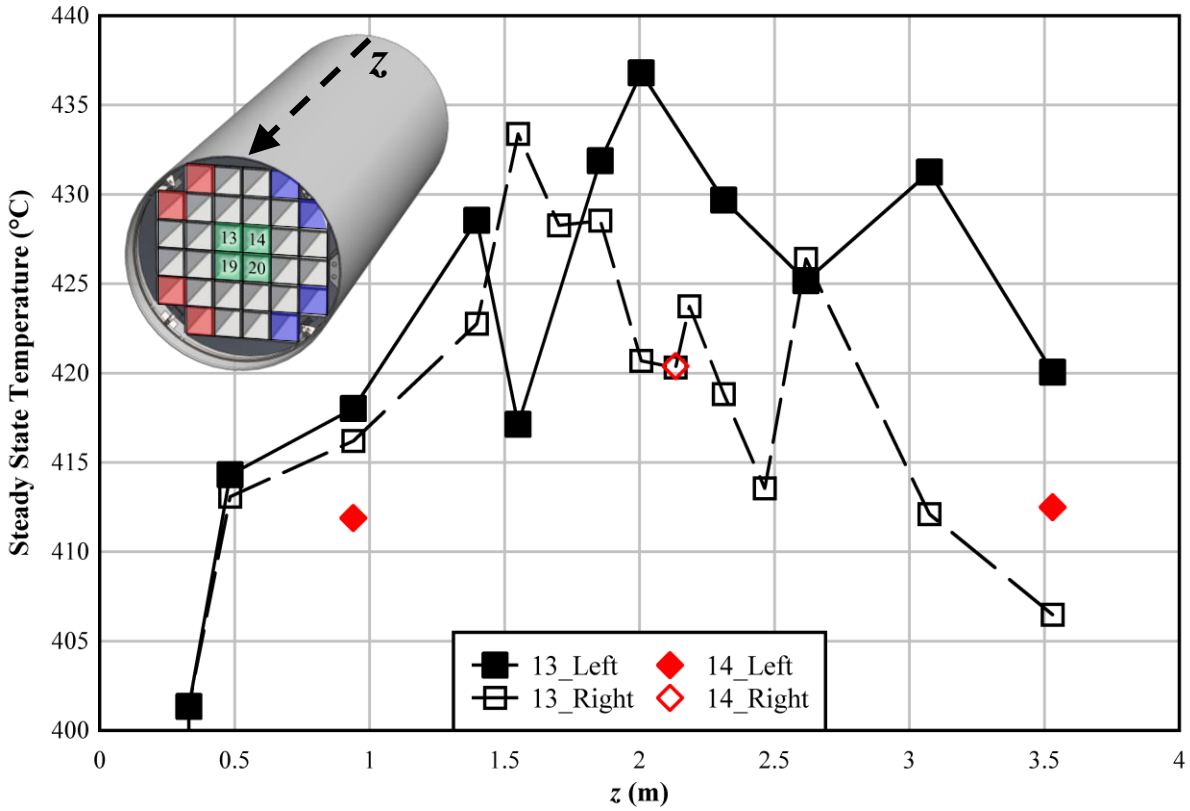

Figure 3.10 Temperature data from a 20.0 kW test is plotted against distance from the bottom of the canister for the heater assemblies in basket cells 13 and 14.

3.4 Heat Loading Configuration

Based on comparisons with modeling and a desire to optimize the load balance across the three electrical phases, a novel 10-10-12 Heat Load Zone (HLZ) pattern was adopted for the CDFD canisters as depicted in Figure 3.11. This loading deviates from that outlined in the Final Safety Analysis Report (FSAR) but allows compensation for operations with heaters and unsealed air instead of spent fuel and helium. Each heater assembly has two heaters, a primary and a backup heater. Only one heater per assembly will be used at a given time. The heaters within a HLZ will be wired in parallel to one phase and neutral.

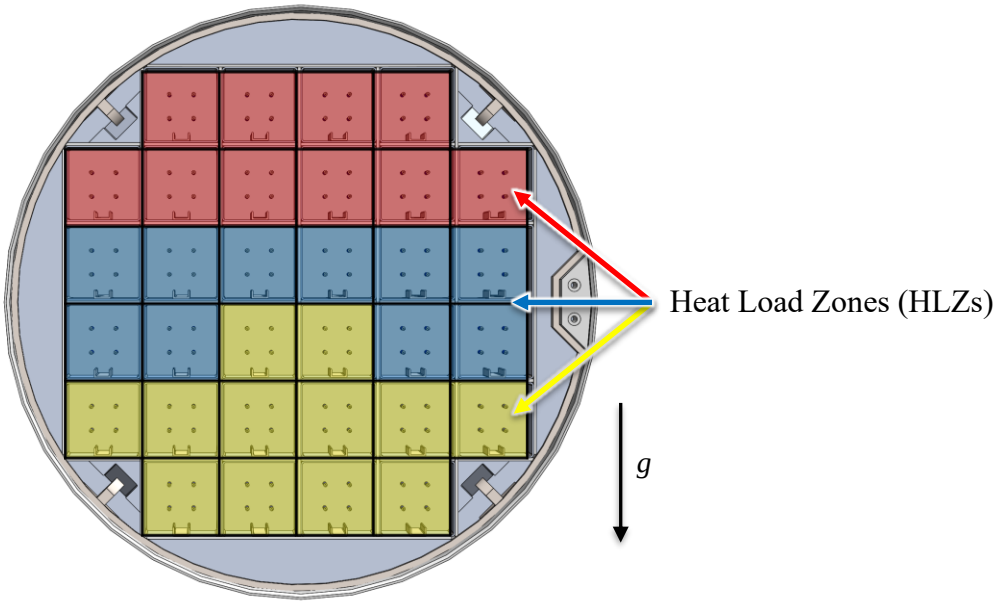

Figure 3.11 Cross-section showing the three Heat Load Zones for the CDFD canisters.

3.4.1 Load Balancing

The distribution of heater power for the 10-10-12 HLZ is given in Table 3.2 for a 40 kW canister. The lower heater assemblies have a both a smaller applied total and assembly heat load in order to bias heat to the top of the shell, again to compensate for the substitution of heaters and operation in air.

Table 3.3 shows the expected resistance, amps, and volts for each of the three electrical phases in a 40 kW canister. The maximum line-to-neutral voltage for this system is 277 V, whereas the line-to-line voltage is the more commonly referenced 480 V service. By biasing the heaters in the 10-10-12 arrangement and applying a lower heat per assembly in zone C, the amperage on each phase is nearly equal, which is a primary goal of load balancing. Although not shown here, the results for a 10 kW canister, or any other heat load, yield similar well balanced electrical circuits for this HLZ configuration.

Table 3.2 HLZs for a 40 kW canister.

Zone	1A	1B	1C	Total
Number of Assemblies	10	10	12	32
Assembly Power (kW)	1.400	1.400	1.000	--
Zone Power (kW)	14.000	14.000	12.000	40

Table 3.3 Electrical values of the three phases for a 40 kW canister.

Zone	1A	1B	1C
R (Ohms)	3.825	3.825	3.1875
I (Amps)	**60.5**	**60.5**	**61.4**
V (Volts)	231.4	231.4	195.6

3.4.2 Thermal Model Comparisons

Figure 3.12 gives a comparison of shell temperatures along the top of the canister for the thermal model loaded with SNF and CDFD heaters at 40 kW on the left. This comparison shows that the predicted performance of the heaters match a canister loaded with SNF to a maximum shell temperature error of about 2% and an average of less than 1% of the SNF shell temperatures.

Similarly, Figure 3.13 shows a comparison of shell temperatures on waist of the SNF and heater canisters on the left. Here, the two models give errors based on the SNF shell temperatures for a maximum of 4% and an average of less than 1%. Finally, the isometric temperature contours on the right of the figures for the SNF canister (Figure 3.12) and the CDFD heater canister (Figure 3.13) appear to give similar overall comparisons as the line probes based on casual inspection.

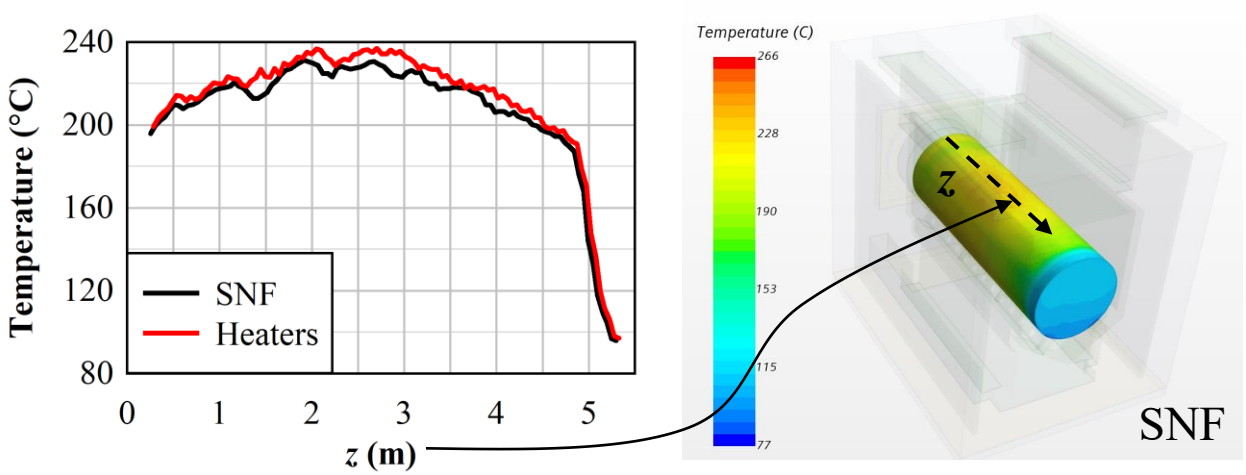

Figure 3.12 Comparison of canister shell temperatures along the top of the canister at 40 kW (left). Isometric temperature contours for a model with SNF (right).

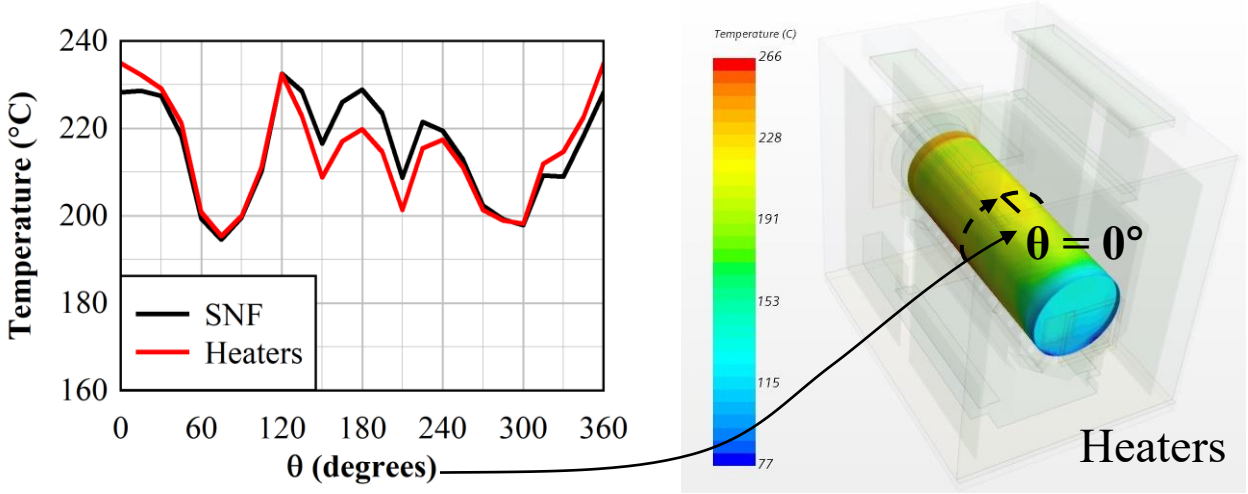

Figure 3.13 Comparison of canister shell temperatures around the waist of the canister (left). Isometric temperature contours for a model with CDFD heaters (right).

4 PROJECT PLANNING

An ISFSI near a marine coastal environment would be ideal to provide realistic conditions for this long-term deposition study. Operating at a remote location such as an ISFSI requires a central hub located on site for power distribution and DAQ. A modified transportation container would fulfill these needs. Remote operation of the test equipment and data transmission from the test site also requires consideration. Locating a host site that can accommodate the network service, power, and testing footprint of the CDFD is crucial to mission success.

4.1 Remote Data Acquisition System

Remote operation of the data acquisition (DAQ) and test control systems are a critical component of the proposed testing. These systems are designed to run autonomously but require periodic verification of operation by operators. In addition, data files will be periodically uploaded to servers for analysis and archival. Figure 4.1 shows a schematic of the major components for the DAQ and test control networking system.

The test equipment is wired to a central DAQ system that also provides test control. Data is collected and stored locally. The DAQ is routed to a virtual private network (VPN) gateway that is redundantly connected to the internet via both cellular (primary connection) and satellite (secondary) modems. This connection to the internet allows the DAQ to both send alerts and alarms to test team members via email and texts as well as upload data files to protected servers. This connection also allows team members to access the DAQ through remote desktop protocol (RDP) and perform corrective or shutdown functions without having to travel to the test site.

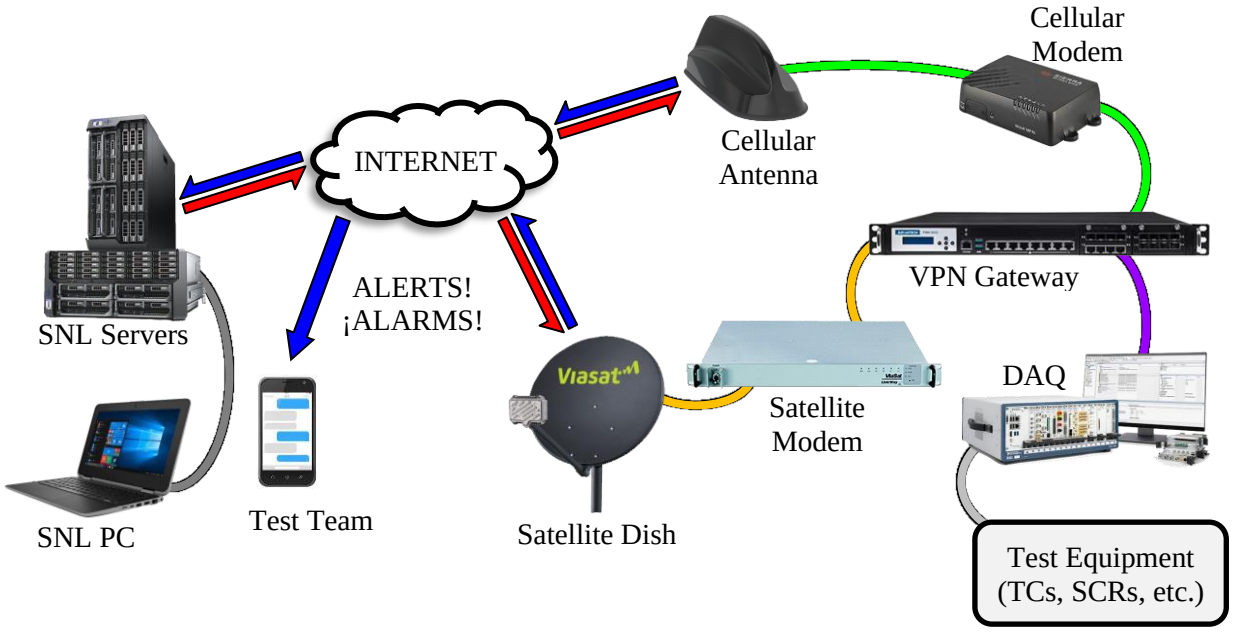

Figure 4.1 Schematic of network architecture for remote operations of the data acquisition and test control systems.

4.2 Power and Instrumentation Skid

The power and instrumentation skid will provide a protected enclosure for power control, instrumentation interfaces, and the remote DAQ system. This unit is comprised of an insulated steel storage container (width × depth × height = 8 × 20 × 8.5 ft.) with a wall-mounted heating, ventilation, and air conditioning (HVAC) unit for climate control. To accommodate clearance and cable management, the final footprint of the power and instrumentation skid is expected to be 10 × 25 ft. The primary power service requirements are estimated to be a total of 80 kW, which allows for continuous use of 50 kW for simulated decay heats (40 and 10 kW) and 15 kW for the remote DAQ, HVAC, and test instrumentation. This load represents 81% of the service capacity. A model of the power and instrumentation skid and its internal components is shown in Figure 4.2. The rear wall containing the power distribution equipment of the as-built power skid is shown in Figure 4.3. Electrical components selected for the power skid are marine grade to withstand the conditions in a coastal environment. Power distribution panels will be placed within a NEMA 3R enclosure for those mounted on the interior. The power disconnect mounted on the exterior will be contained within a NEMA 4X enclosure to provide enhanced corrosion protection.

The power and instrumentation skid will also host the ambient aerosol sampling and atmospheric monitoring equipment described in Section 2.6. The aerosol sampling cabinet will be mounted to the exterior of the power skid, facing the same direction as the AHSM air inlets. The aerosol sampling cabinet is pictured in Figure 4.2.

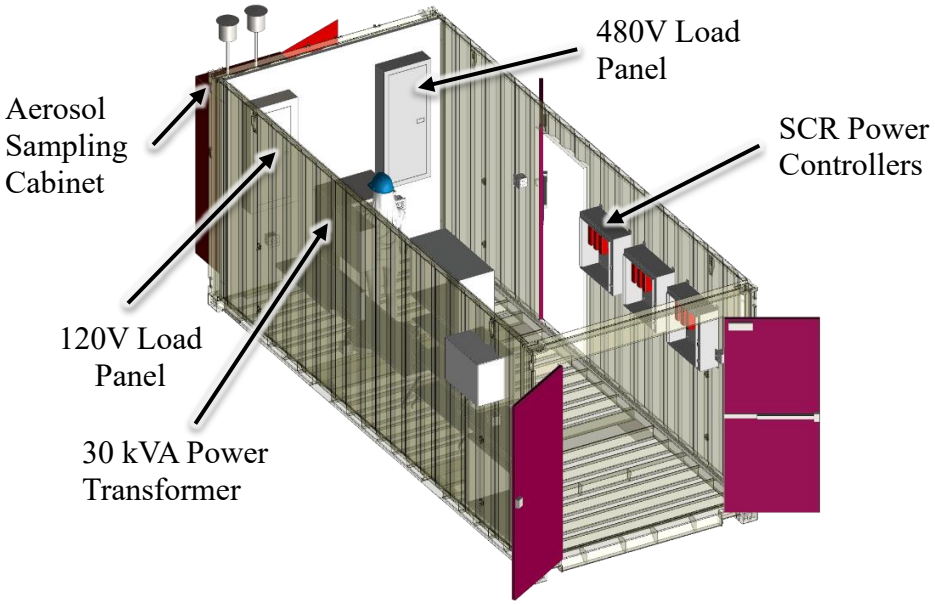

Figure 4.2 CAD model of the power and instrumentation skid for power distribution to the test canisters and remote data acquisition.

Figure 4.3 Rear wall of the power and instrumentation skid showing the 120 V load panel for data acquisition and accessory equipment power (left), 30 kVA power transformer (center), and 480 V load panel for heater assembly power (right).

4.3 Testing Layout

Three different footprints of the test equipment are shown in the overhead view in Figure 4.4. The first width by length of 17.1 × 13.4 m (56 × 44 ft.) in red is the tightest envelope possible around the test equipment with a canister extracted. The next window in yellow of 22.9 × 19.5 m (75 × 64 ft.) is the smallest footprint considered to be operationally feasible. Assuming this is the footprint of the concrete pad, these dimensions accommodate the approach of the transfer skid on the concrete. Finally, a footprint of 30.5 × 25.9 m (100 × 85 ft.) in green represents the recommended footprint for CDFD operations. The height for all three footprints is based on the height of the AHSMs of 6.1 m (20 ft.). Figure 4.5 provides an isometric view of the testing setup and layout during normal testing operations.

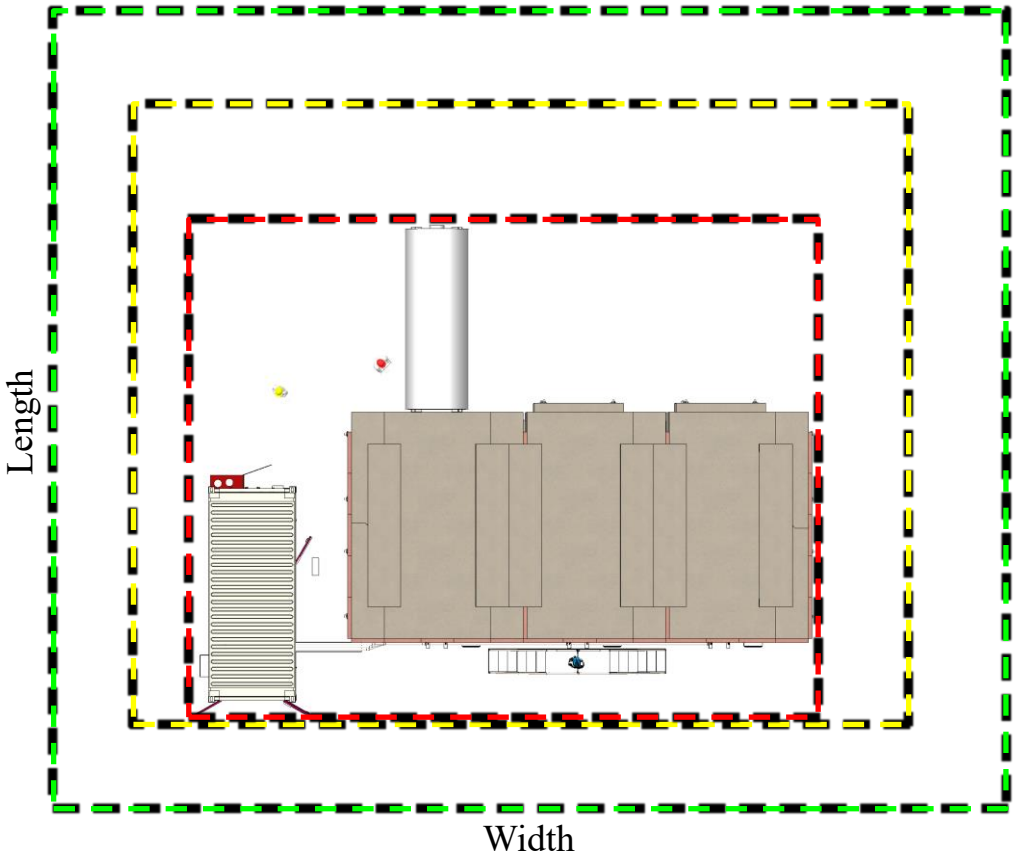

Figure 4.4 **Footprints of the CDFD test equipment (red), minimum operational window (yellow), and recommended operational window (green).**

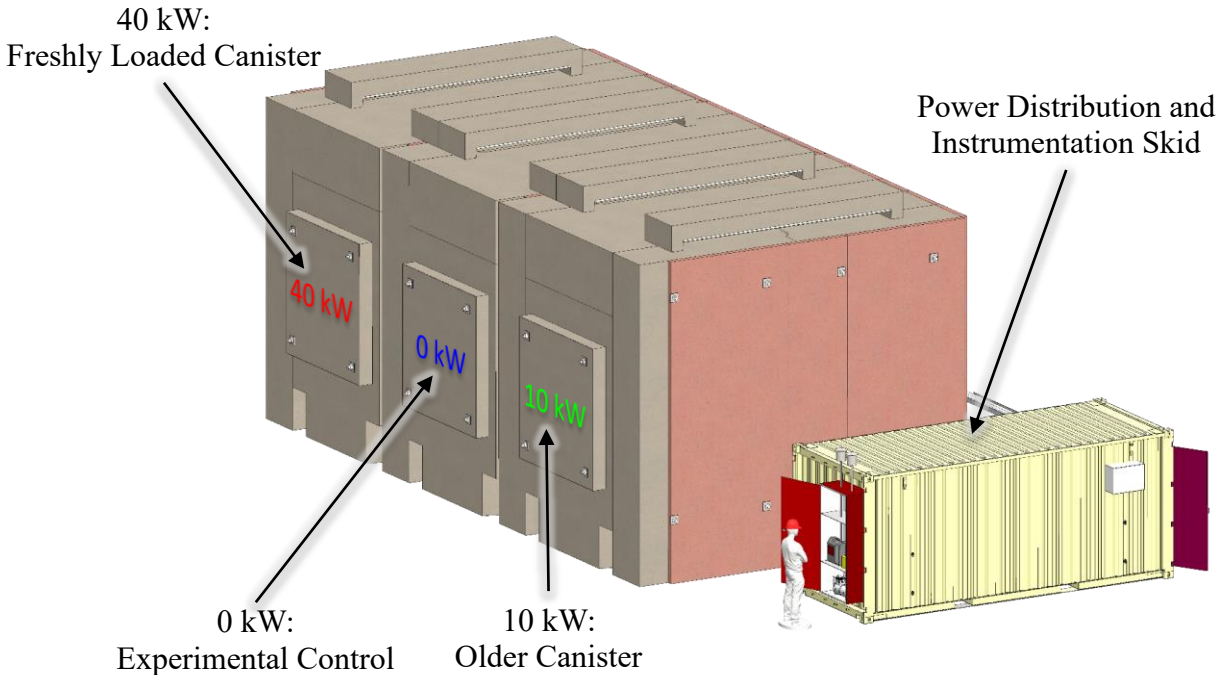

Figure 4.5 **Isometric view of the CDFD testing layout.**

5 SUMMARY

This report provides updates on the high-level test plan [Lindgren *et al*., 2020] and previous status update [Fascitelli *et al*., 2022] for the CDFD project, specifically for evaluating surface deposition on DSCs and the continued work that has been conducted to date. The goal of the testing is to collect highly defensible and detailed surface deposition measurements of dry canisters in a marine coastal environment to guide CISCC research. To facilitate surface sampling, the otherwise highly prototypic DCSS will not contain SNF but rather will be electrically heated to mimic the prototypic decay heat and thermal environment.

The outer top cover of the dry shielded canister will be modified such that it can be mechanically attached to the DSC shell with the use of set screw fixtures and will serve as the only cover installed. The inner top cover and shield plug will not be installed. The top outer cover is intended to be installed and left in place through the duration of testing but can be removed if maintenance to the heater assemblies is required.

The concrete AHSM vaults will also be modified to accommodate CDFD operations. A rear hatch will be cut in the back wall of the vault to gain access to power and instrumentation junction boxes mounted to the modified outer top cover. Internal and external temperature sensor and heater power wiring will exit the vault through this access opening. Insulation will be added to the AHSMs to provide near-adiabatic boundary conditions for each system. A thermal break between adjacent vaults is particularly important to prevent the high-powered test from influencing the adjacent lower-powered test and unpowered control. Insulating the exterior side and back walls serve to provide near-adiabatic boundary conditions and improve modeling validation.

Preliminary heater tests have been conducted at heat loads ranging from 4.8 to 35 kW. These tests have indicated that the electric heaters are appropriate surrogates for spent nuclear fuel and can adequately heat the dry shielded canister. Initial testing has also informed thermal modeling parameters and facilitated the development of a more accurate thermal model of the system. Thermal modeling has informed the testing team of an optimal heat load configuration for the three phases of power that will most closely match the thermal profile of a canister loaded with spent nuclear fuel.

Final heater assemblies featuring two U-tube heaters have been designed with an emphasis on longevity and are currently being instrumented with thermocouples in preparation for further testing of the CDFD canisters. Each heater in the assembly will receive one type-K thermocouple located at an axial region of interest. These regions primarily include locations on the canister surface where a surface sampling will occur. Type-T TCs will be used to mark the sampling grids and be attached with shim stock.

The power and instrumentation skid has been designed for a coastal host site. This modified transportation container will provide a weather-tight, climate-controlled enclosure for the power distribution and DAQ system. A cabinet for the ambient aerosol sampling and atmospheric monitoring equipment will be mounted to the exterior of the power skid.

Mockup structures of the canister transfer skid and Advanced Horizontal Storage Module rear wall were designed and built at the NEWC in SNL. These mockups provide a realistic setting for the surface sampling and testing teams to establish proper operational procedures and identify any limitations or obstacles of the testing setup and equipment. Accessibility, limitations, and specialized equipment needed during testing and surface sampling will be identified and finalized through practice with the test mockups. Staged field testing has been fulfilled, with more planned in the future.

5.1 Future Work

Prior to canister deployment and field testing, SNL will continue testing CDFD hardware such as the electrical heater assemblies and the power skid. Slight modifications of the heater assemblies need to be made to ensure proper fit into the basket cells. After instrumenting the assemblies with thermocouples, the assemblies will be loaded into the canisters and functional testing will begin. Tests ranging from 3.2 to 40.0 kW are planned for each canister. These tests will continue to support the thermal modeling team and help to understand and anticipate the performance of the new test and heat load configuration. After final modifications to the power skid have been made, the skid will be relocated to SNL's Building 6630 where the test canisters are located. The power skid is planned to be outfitted with all the necessary data acquisition and power distribution equipment needed to control each canister at once.

SNL will continue troubleshooting and debugging the remote DAQ system. Interruptions of the connection (e.g., inclement weather, power outages) to SNL servers while the CDFD test is deployed at a remote test site is expected. These interruptions must not cause damage to the hardware and must be recoverable. Identifying weak points or functions susceptible to failure for the remote DAQ system is critical to mission success. Initiating, stopping, and gathering data from tests remotely will be rehearsed during the functional testing of each test canister.

The CDFD sampling team plans to perform additional staged surface sampling tests. The sampling team will continue to use the transfer skid mockup to rehearse and refine the sampling procedures and techniques. Increasing the accuracy of their measurements, or at the very least, understanding the amount of uncertainty from their collection is essential for producing meaningful surface deposition data.

The CDFD testing team plans to deploy the ambient aerosol sizing and characterization equipment at potential host sites of interest. Potential host sites can be evaluated based on the amount of salt particles in the ambient air and other atmospheric conditions. A criterion for aerosol composition and ambient salt load must be determined prior to selecting a host site. Given the ambient aerosol characterization data and logistical considerations for the project (e.g., shipping components, travel, expense) a decision for the CDFD host site will be made. Once this decision is agreed upon by the testing team and project controllers, the project can progress towards canister deployment.

6 REFERENCES

Bryan, C., A. Knight, R. Schaller, S.G. Durbin, B. Nation, and P. Jensen, "Surface Sampling Techniques for the Canister Deposition Field Demonstration," SAND2021-3329 R, Sandia National Laboratories, Albuquerque, NM, March 2021.

Bryan, C., A. Knight, B. Nation, T. Montoya, E. Karasz, R. Katona, and R. Schaller, "FY21 Status Report: SNF Interim Storage Canister Corrosion and Surface Environment Investigations," SAND2021-12903 R, Sandia National Laboratories, Albuquerque, NM, September 2021.

Fascitelli, D.G., S.G. Durbin, S.R. Suffield, J.A. Fort and B.J. Jensen, "Status Update for the Canister Deposition Field Demonstration," SAND2022-8167 R, Sandia National Laboratories, Albuquerque, NM, June 2022.

Jensen, P.J., S. Suffield, C.L. Grant, C. Spitz, B. Hanson, S. Ross, S. Durbin, C. Bryan, and S. Saltzstein, "Preliminary Modeling of Chloride Deposition on Spent Nuclear Fuel Canisters in Dry Storage Relevant to Stress Corrosion Cracking," SAND2021-3570 J, Pacific Northwest National Laboratory, Richland, WA, 2021.

Knight, A., R. Schaller, B. Nation, S. Durbin, and C. Bryan, "FY22 Update: Development of Surface Sampling Techniques for the Canister Deposition Field Demonstration," SAND2022-4533 R, Sandia National Laboratories, Albuquerque, New Mexico, April 2022.

Knight, A.W., D.G. Fascitelli, C.R. Bryan, S.G. Durbin, S. Verma, M. Maguire, and B. Nation, "FY23 Update: Surface Sampling Activities for the Canister Deposition Field Demonstration," SAND2023-01875 R, Sandia National Laboratories, Albuquerque, NM, April 2023.

Lindgren, E.R., S.G. Durbin, S.R. Suffield, and J.A. Fort, "Preliminary Test Design and Plan for a Canister Deposition Field Demonstration," SAND2020-13075 R, Sandia National Laboratories, Albuquerque, NM, November 2020.

Lindgren, E.R., S.G. Durbin, S.R. Suffield, and J.A. Fort, "Status Update for the Canister Deposition Field Demonstration," SAND2021-6471 R, Sandia National Laboratories, Albuquerque, NM, May 2021.

Pulido, R.J.M., A. Taconi, A. Salazar III, R.E. Fasano, R.W. Williams, B. Baigas, and S.G Durbin, "Response of a Pressurized Water Reactor Dashpot Region to Commercial Drying Cycles," SAND2022-3813 R, Sandia National Laboratories, Albuquerque, NM, April 2022.

Transnuclear Inc., "Advanced NUHOMS System Updated Final Safety Analysis Report (UFSAR)", Rev. 7, August 2016.

Transnuclear Inc., "NUHOMS® HD System Safety Analysis Report (FSAR)", Rev. 6, September 2017.

Schindelholz, E., C. Bryan, and C. Alexander, "FY17 Status Report: Research on Stress Corrosion Cracking of SNF Interim Storage Canisters," SAND2017-10338R, Sandia National Laboratories, Albuquerque, NM, August 2017.

U.S.NRC, "Materials Aging Issues and Aging Management for Extended Storage and Transportation of Spent Nuclear Fuel", NUREG/CR-7116, September 2011.

This page is intentionally left blank.


Sandia National Laboratories